REVIEW Communicated by Dan Johnston

The NEURON Simulation Environment

M. L. Hines
Department of Computer Science and Neuroengineering and Neuroscience Center, Yale University, New Haven, CT 06520, U.S.A.

N. T. Carnevale
Psychology Department, Yale University, New Haven, CT 06520, U.S.A.

The moment-to-moment processing of information by the nervous system involves the propagation and interaction of electrical and chemical signals that are distributed in space and time. Biologically realistic modeling is needed to test hypotheses about the mechanisms that govern these signals and how nervous system function emerges from the operation of these mechanisms. The NEURON simulation program provides a powerful and flexible environment for implementing such models of individual neurons and small networks of neurons. It is particularly useful when membrane potential is nonuniform and membrane currents are complex. We present the basic ideas that would help informed users make the most efficient use of NEURON.

1 Introduction

NEURON (Hines, 1984, 1989, 1993, 1994) provides a powerful and flexible environment for implementing biologically realistic models of electrical and chemical signaling in neurons and networks of neurons. This article describes the concepts and strategies that have guided the design and implementation of this simulator, with emphasis on those features that are particularly relevant to its most efficient use.

1.1 The Problem Domain. Information processing in the brain results from the spread and interaction of electrical and chemical signals within and among neurons. This involves nonlinear mechanisms that span a wide range of spatial and temporal scales (Carnevale & Rosenthal, 1992) and are constrained to operate within the intricate anatomy of neurons and their interconnections. Consequently the equations that describe brain mechanisms generally do not have analytical solutions, and intuition is not a reliable guide to understanding the working of the cells and circuits of the brain. Furthermore, these nonlinearities and spatiotemporal complexities are quite unlike those that are encountered in most nonbiological systems,

so the utility of many quantitative and qualitative modeling tools that were developed without taking these features into consideration is severely limited.

NEURON is designed to address these problems by enabling both the convenient creation of biologically realistic quantitative models of brain mechanisms and the efficient simulation of the operation of these mechanisms. In this context the term *biological realism* does not mean "infinitely detailed." Instead, it means that the choice of which details to include in the model and which to omit are at the discretion of the investigator who constructs the model, and not forced by the simulation program.

To the experimentalist, NEURON offers a tool for cross-validating data, estimating experimentally inaccessible parameters, and deciding whether known facts account for experimental observations. To the theoretician, it is a means for testing hypotheses and determining the smallest subset of anatomical and biophysical properties that is necessary and sufficient to account for particular phenomena. To the student in a laboratory course, it provides a vehicle for illustrating and exploring the operation of brain mechanisms in a simplified form that is more robust than the typical "wet lab" experiment. For the experimentalist, theoretician, and student alike, a powerful simulation tool such as NEURON can be an indispensable aid to developing the insight and intuition that is needed if one is to discover the order hidden within the intricacy of biological phenomena, the order that transcends the complexity of accident and evolution.

1.2 Experimental Advances and Quantitative Modeling. Experimental advances drive and support quantitative modeling. Over the past two decades, the field of neuroscience has seen striking developments in experimental techniques, among them the following:

- High-quality electrical recording from neurons in vitro and in vivo using patch clamp.
- Multiple impalements of visually identified cells.
- Simultaneous intracellular recording from paired pre- and postsynaptic neurons.
- Simultaneous measurement of electrical and chemical signals.
- Multisite electrical and optical recording.
- Quantitative analysis of anatomical and biophysical properties from the same neuron.
- Photolesioning of cells.
- Photorelease of caged compounds for spatially precise chemical stimulation.

- New drugs such as channel blockers and receptor agonists and antagonists.
- Genetic engineering of ion channels and receptors.
- Analysis of messenger RNA and biophysical properties from the same neuron.
- "Knockout" mutations.

These and other advances are responsible for impressive progress in the definition of the molecular biology and biophysics of receptors and channels; the construction of libraries of identified neurons and neuronal classes that have been characterized anatomically, pharmacologically, and biophysically; and the analysis of neuronal circuits involved in perception, learning, and sensorimotor integration.

The result is a data avalanche that catalyzes the formulation of new hypotheses of brain function, while at the same time serving as the empirical basis for the biologically realistic quantitative models that must be used to test these hypotheses. Following are some examples from the large list of topics that have been investigated through the use of such models:

- The cellular mechanisms that generate and regulate chemical and electrical signals (Destexhe, Contreras, Steriade, Sejnowski, & Huguenard, 1996; Jaffe et al., 1994).
- Drug effects on neuronal function (Lytton & Sejnowski, 1992).
- Presynaptic (Lindgren & Moore, 1989) and postsynaptic (Destexhe & Sejnowski, 1995; Traynelis, Silver, & Cull-Candy, 1993) mechanisms underlying communication between neurons.
- Integration of synaptic inputs (Bernander, Douglas, Martin, & Koch, 1991; Cauller & Connors, 1992).
- Action potential initiation and conduction (Häusser, Stuart, Racca, & Sakmann, 1995; Hines & Shrager, 1991; Mainen, Joerges, Huguenard, & Sejnowski, 1995).
- Cellular mechanisms of learning (Brown, Zador, Mainen, & Claiborne, 1992; Tsai, Carnevale, & Brown, 1994a).
- Cellular oscillations (Destexhe, Babloyantz, & Sejnowski, 1993a; Lytton, Destexhe, & Sejnowski, 1996).
- Thalamic networks (Destexhe, McCormick, & Sejnowski, 1993b; Destexhe, Contreras, Sejnowski, & Steriade, 1994).
- Neural information encoding (Hsu et al., 1993; Mainen & Sejnowski, 1995; Softky, 1994).

2 Overview of NEURON

NEURON is intended to be a flexible framework for handling problems in which membrane properties are spatially inhomogeneous and where membrane currents are complex. Since it was designed specifically to simulate the equations that describe nerve cells, NEURON has three important advantages over general-purpose simulation programs. First, the user is not required to translate the problem into another domain, but instead is able to deal directly with concepts that are familiar at the neuroscience level. Second, NEURON contains functions that are tailored specifically for controlling the simulation and graphing the results of real neurophysiological problems. Third, its computational engine is particularly efficient because of the use of special methods and tricks that take advantage of the structure of nerve equations (Hines, 1984; Mascagni, 1989).

The general domain of nerve simulation, however, is still too large for any single program to deal optimally with every problem. In practice, each program has its origin in a focused attempt to solve a restricted class of problems. Both speed of simulation and the ability of the user to maintain conceptual control degrade when any program is applied to problems outside the class for which it is best suited.

NEURON is computationally most efficient for problems that range from parts of single cells to small numbers of cells in which cable properties play a crucial role. In terms of conceptual control, it is best suited to tree-shaped structures in which the membrane channel parameters are approximated by piecewise linear functions of position. Two classes of problems for which it is particularly useful are those in which it is important to calculate ionic concentrations and those where one needs to compute the extracellular potential just next to the nerve membrane. It is especially capable for investigating new kinds of membrane channels since they are described using a high-level neuron model description language (NMODL) (Moore & Hines, 1996), which allows the expression of models in terms of kinetic schemes or sets of simultaneous differential and algebraic equations. To maintain efficiency, user-defined mechanisms in NMODL are automatically translated into C, compiled, and linked into the rest of NEURON.

The flexibility of NEURON comes from a built-in object-oriented interpreter, which is used to define the morphology and membrane properties of neurons, control the simulation, and establish the appearance of a graphical interface. The default graphical interface is suitable for exploratory simulations involving the setting of parameters, control of voltage and current stimuli, and graphing variables as a function of time and position.

Simulation speed is excellent since membrane voltage is computed by an implicit integration method optimized for branched structures (Hines, 1984). The performance of NEURON degrades very slowly with increased complexity of morphology and membrane mechanisms, and it has been applied to very large network models: 10^4 cells with six compartments each,

for a total of 10^6 synapses in the net (T. Sejnowski, personal communication, March 29, 1996).

3 Mathematical Basis

Strategies for numerical solution of the equations that describe chemical and electrical signaling in neurons have been discussed in many places. Elsewhere we have briefly presented an intuitive rationale for the most commonly used methods (Hines & Carnevale, 1995). Here we start from this base and proceed to address those aspects that are most pertinent to the design and application of NEURON.

3.1 The Cable Equation. The application of cable theory to the study of electrical signaling in neurons has a long history, which is briefly summarized elsewhere (Rall, 1989). The basic computational task is to solve numerically the cable equation

$$\frac{\partial V}{\partial t} + I(V, t) = \frac{\partial^2 V}{\partial x^2}, \tag{3.1}$$

which describes the relationship between current and voltage in a one-dimensional cable. The branched architecture typical of most neurons is incorporated by combining equations of this form with appropriate boundary conditions.

Spatial discretization of this partial differential equation is equivalent to reducing the spatially distributed neuron to a set of connected compartments. The earliest example of a multicompartmental approach to the analysis of dendritic electrotonus was provided by Rall (1964).

Spatial discretization produces a family of ordinary differential equations of the form

$$c_j \frac{dv_j}{dt} + i_{ion_j} = \sum_k \frac{v_k - v_j}{r_{jk}}. \tag{3.2}$$

Equation 3.2 is a statement of Kirchhoff's current law, which asserts that net transmembrane current leaving the jth compartment must equal the sum of axial currents entering this compartment from all sources (see Figure 1). The left-hand side of equation 3.2 is the total membrane current, which is the sum of capacitive and ionic components. The capacitive component is $c_j dv_j/dt$, where c_j is the membrane capacitance of the compartment. The ionic component i_{ion_j} includes all currents through ionic channel conductances. The right-hand side of equation 3.2 is the sum of axial currents that enter this compartment from its adjacent neighbors. Currents injected through a microelectrode would be added to the right-hand side. The sign conventions for current are as follows: outward transmembrane current is positive; axial

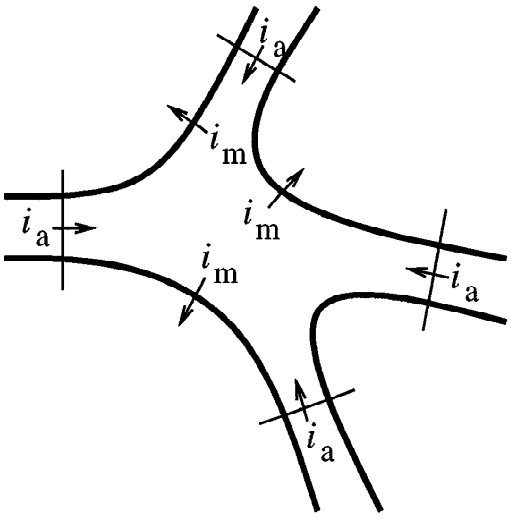

Figure 1: The net current entering a region must equal zero.

current flow into a region is positive; positive injected current drives v_j in a positive direction.

Equation 3.2 involves two approximations. First, axial current is specified in terms of the voltage drop between the centers of adjacent compartments. The second approximation is that spatially varying membrane current is represented by its value at the center of each compartment. This is much less drastic than the often-heard statement that a compartment is assumed to be "isopotential." It is far better to picture the approximation in terms of voltage varying linearly between the centers of adjacent compartments. Indeed, the linear variation in voltage is implicit in the usual description of a cable in terms of discrete electrical equivalent circuits.

If the compartments are of equal size, it is easy to use Taylor's series to show that both of these approximations have errors proportional to the square of compartment length. Thus, replacing the second partial derivative by its central difference approximation introduces errors proportional to Δx^2, and doubling the number of compartments reduces the error by a factor of four.

It is often not convenient for the size of all compartments to be equal. Unequal compartment size might be expected to yield simulations that are only first-order accurate. However, comparison of simulations in which unequal compartments are halved or quartered in size generally reveals a

second-order reduction of error. A rough rule of thumb is that simulation error is proportional to the square of the size of the largest compartment.

The first of two special cases of equation 3.2 that we wish to discuss allows us to recover the usual parabolic differential form of the cable equation. Consider the interior of an unbranched cable with constant diameter. The axial current consists of two terms involving compartments with the natural indices $j-1$ and $j+1$, that is,

$$c_j \frac{dv_j}{dt} + i_{ion_j} = \frac{v_{j-1} - v_j}{r_{j-1,j}} + \frac{v_{j+1} - v_j}{r_{j,j+1}}.$$

If the compartments have the same length Δx and diameter d, then the capacitance of a compartment is $C_m \pi d \Delta x$, and the axial resistance is $R_a \Delta x / \pi (d/2)^2$. C_m is called the specific capacitance of the membrane, which is generally taken to be 1 μf/cm^2. R_a is the axial resistivity, which has different reported values for different cell classes (e.g., 35.4 Ω cm for squid axon). Equation 3.2 then becomes

$$C_m \frac{dv_j}{dt} + i_j = \frac{d}{4R_a} \frac{v_{j+1} - 2v_j + v_{j-1}}{\Delta x^2},$$

where we have replaced the total ionic current i_{ion_j} with the current density i_j. The right-hand term, as $\Delta x \to 0$, is just $\partial^2 v / \partial x^2$ at the location of the now-infinitesimal compartment j.

The second special case of equation 3.2 allows us to recover the boundary condition. This is an important exercise since naive discretizations at the ends of the cable have destroyed the second-order accuracy of many simulations. Nerve boundary conditions are that no axial current flows at the end of the cable; the end is sealed. This is implicit in equation 3.2, where the right-hand side consists of only the single term $(v_{j-1} - v_j)/r_{j-1,j}$ when compartment j lies at the end of an unbranched cable.

3.2 Spatial Discretization in a Biological Context: Sections and Segments. Every nerve simulation program solves for the longitudinal spread of voltage and current by approximating the cable equation as a series of compartments connected by resistors (see Figure 4 and equation 3.2). The sum of all the compartment areas is the total membrane area of the whole nerve. Unfortunately, it is usually not clear at the outset how many compartments should be used. Both the accuracy of the approximation and the computation time increase as the number of compartments used to represent the cable increases. When the cable is "short," a single compartment can be made to represent the entire cable adequately. For long cables or highly branched structures, it may be necessary to use a large number of compartments.

This raises the question of how best to manage all the parameters that exist within these compartments. Consider membrane capacitance, which

has a different value in each compartment. Rather than specify the capacitance of each compartment individually, it is better to deal in terms of a single specific membrane capacitance that is constant over the entire cell and have the program compute the values of the individual capacitances from the areas of the compartments. Other parameters such as diameter or channel density may vary widely over short distances, so the graininess of their representation may have little to do with numerically adequate compartmentalization.

Although NEURON is a compartmental modeling program, the specification of biological properties (neuron shape and physiology) has been separated from the numerical issue of compartment size. What makes this possible is the notion of a section, which is a continuous length of unbranched cable. Although each section is ultimately discretized into compartments, values that can vary with position along the length of a section are specified in terms of a continuous parameter that ranges from 0 to 1 (normalized distance). In this way, section properties are discussed without regard to the number of segments used to represent it. This makes it easy to trade off between accuracy and speed, and enables convenient verification of the numerical correctness of simulations.

Sections are connected together to form any kind of branched tree structure. Figure 2 illustrates how sections are used to represent biologically significant anatomical features. The top of this figure is a cartoon of a neuron with a soma that gives rise to a branched dendritic tree and an axon hillock connected to a myelinated axon. Each biologically significant component of this cell has its counterpart in one of the sections of the NEURON model, as shown in the bottom of Figure 2: the cell body (*Soma*), axon hillock (*AH*), myelinated internodes (I_i), nodes of Ranvier (N_i), and dendrites (D_i). Sections allow this kind of functional and anatomical parcellation of the cell to remain foremost in the mind of the person who constructs and uses a NEURON model.

To accommodate requirements for numerical accuracy, NEURON represents each section by one or more segments of equal length (see Figures 3 and 4). The number of segments is specified by the parameter `nseg`, which can have a different value for each section.

At the center of each segment is a node, the location where the internal voltage of the segment is defined. The transmembrane currents over the entire surface area of a segment are associated with its node. The nodes of adjacent segments are connected by resistors.

It is crucial to realize that the location of the second-order correct voltage is not at the edge of a segment but rather at its *center*, that is, at its node. This is the discretization method employed by NEURON. To allow branching and injection of current at the precise ends of a section while maintaining second-order correctness, extra voltage nodes that represent compartments with zero area are defined at the section ends. It is possible to achieve second-order accuracy with sections whose end nodes have

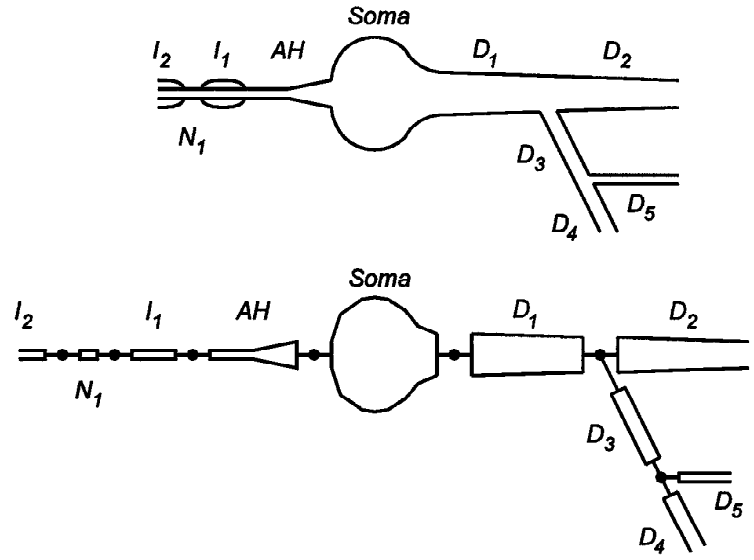

Figure 2: (Top) Cartoon of a neuron indicating the approximate boundaries between biologically significant structures. The left-hand side of the cell body (*Soma*) is attached to an axon hillock (*AH*) that drives a myelinated axon (myelinated internodes I_i alternating with nodes of Ranvier N_i). From the right-hand side of the cell body originates a branched dendritic tree (D_i). (Bottom) How sections would be employed in a NEURON model to represent these structures.

nonzero area compartments. However, the areas of these terminal compartments would have to be exactly half that of the internal compartments, and extra complexity would be imposed on administration of channel density at branch points.

Based on the position of the nodes, NEURON calculates the values of internal model parameters such as the average diameter, axial resistance, and compartment area that are assigned to each segment. Figures 3 and 4 show how an unbranched portion of a neuron, called a neurite (see Figure 3A), is represented by a section with one or more segments. Morphometric analysis generates a series of diameter measurements whose centers lie on the midline of the neurite (the thin axial line in Figure 3B). These measurements and the path lengths between their centers are the dimensions of the section, which can be regarded as a chain of truncated cones or frusta (see Figure 3C).

Distance along the length of a section is discussed in terms of the normalized position parameter x. That is, one end of the section corresponds to

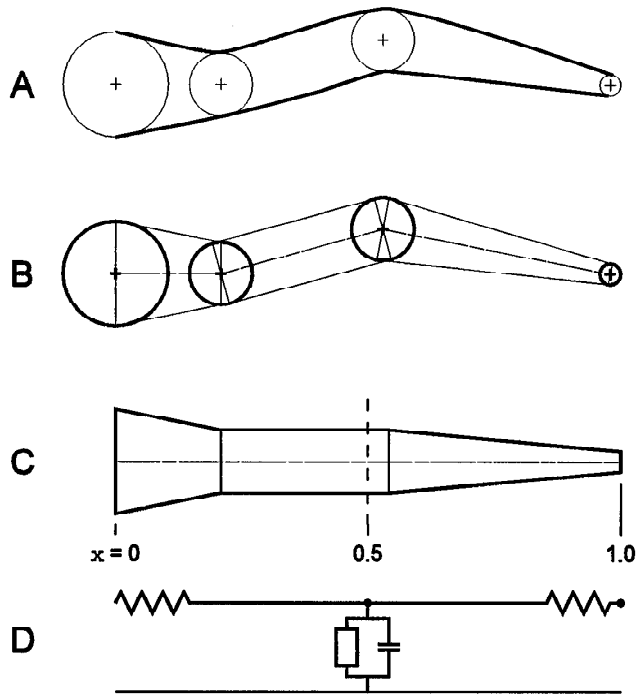

Figure 3: (A) Cartoon of an unbranched neurite (thick lines) that is to be represented by a section in a NEURON model. Computer-assisted morphometry generates a file that stores successive measurements of diameter (thin circles) centered at *x*, *y*, *z* coordinates (thin crosses). (B) Each adjacent pair of diameter measurements (thick circles) becomes the parallel faces of a truncated cone or frustum, the height of which is the distance between the measurement locations. The outline of each frustum is shown with thin lines, and a thin centerline passes through the central axis of the chain of solids. (C) The centerline has been straightened so the faces of adjacent frusta are flush with each other. The scale underneath the figure shows the distance along the midline of the section in terms of the normalized position parameter x. The vertical dashed line at $x = 0.5$ divides the section into two halves of equal length. (D) Electrical equivalent circuit of the section as represented by a single segment ($nseg = 1$). The open rectangle includes all mechanisms for ionic (noncapacitive) transmembrane currents.

$x = 0$ and the other end to $x = 1$. In Figure 3C these locations are depicted as being on the left- and right-hand ends of the section. The locations of the nodes and the boundaries between segments are conveniently specified

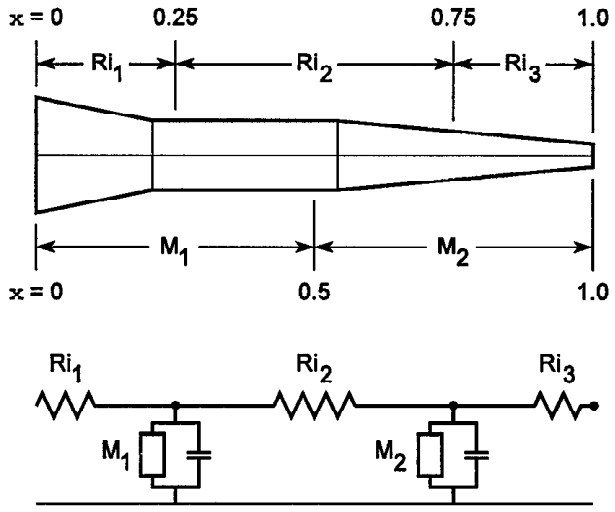

Figure 4: How the neurite of Figure 3 would be represented by a section with two segments (nseg = 2). Now the electrical equivalent circuit (bottom) has two nodes. The membrane properties attached to the first and second nodes are based on neurite dimensions and biophysical parameters over the x intervals [0, 0.5] and [0.5, 1], respectively. The three axial resistances are computed from the cytoplasmic resistivity and neurite dimensions over the x intervals [0, 0.25], [0.25, 0.75], and [0.75, 1].

in terms of this normalized position parameter. In general, a section has nseg segments that are demarcated by evenly spaced boundaries at intervals of 1/nseg. The nodes at the centers of these segments are located at $x = (2i-1)/2\,\mathrm{nseg}$ where *i* is an integer in the range [1, nseg]. As we shall see later, x is also used in specifying model parameters or retrieving state variables that are a function of position along a section (see section 4.4).

The special importance of x and nseg lies in the fact that they free the user from having to keep track of the correspondence between segment number and position on the nerve. In early versions of NEURON, all nerve properties were stored in vector variables where the vector index was the segment number. Changing the number of segments was an error-prone and laborious process that demanded a remapping of the relationship between the user's mental image of the biologically important features of the model, on the one hand, and the implementation of this model in a digital computer, on the other. The use of x and nseg insulates the user from the most inconvenient aspects of such low-level details.

When nseg = 1 the entire section is lumped into a single compartment. This compartment has only one node, which is located midway along its length, at x = 0.5 (see Figures 3C and D). The integral of the surface area over the entire length of the section ($0 \leq x \leq 1$) is used to calculate the membrane properties associated with this node. The values of the axial resistors are determined by integrating the cytoplasmic resistivity along the paths from the ends of the section to its midpoint (dashed line in Figure 3C). The left- and right-hand axial resistances of Figure 3D are evaluated over the x intervals [0, 0.5] and [0.5, 1], respectively.

Figure 4 shows what happens when nseg = 2. Now NEURON breaks the section into two segments of equal length that correspond to x intervals [0, 0.5] and [0.5, 1]. The membrane properties over these intervals are attached to the nodes at 0.25 and 0.75, respectively. The three axial resistors Ri_1, Ri_2, and Ri_3 are determined by integrating the path resistance over the x intervals [0, 0.25], [0.25, 0.75], and [0.75, 1].

3.3 Integration Methods. Spatial discretization reduced the cable equation, a partial differential equation with derivatives in space and time, to a set of ordinary differential equations with first-order derivatives in time. Selection of an integration method to solve these equations is guided by concerns of stability, accuracy, and efficiency (Hines & Carnevale, 1995).

NEURON offers the user a choice of two stable implicit integration methods: backward Euler and a variant of Crank-Nicholson (C-N). Backward Euler is the default because of its robust numerical stability properties. Backward Euler can be used with extremely large time steps in order to find the steady-state solution for a linear ("passive") system. It produces good qualitative results even with large time steps, and it works even if some or all of the equations are strictly algebraic relations among states.

A more accurate method for small time steps is available by setting the global parameter secondorder to 2. NEURON then uses a variant of the C-N method, in which numerical error is proportional to Δt^2.

Both of these are implicit integration methods, in which all current balance equations must be solved simultaneously. The backward Euler algorithm does not resort to iteration to deal with nonlinearities, since its numerical error is proportional to Δt anyway. The special feature of the C-N variant is its use of a staggered time step algorithm to avoid iteration of nonlinear equations (see section 3.3.1). This converts the current balance part of the problem to one that requires only the solution of simultaneous linear equations.

Although the C-N method is formally stable, it is sometimes plagued by spurious large-amplitude oscillations (see Hines and Carnevale, 1995, Figure 7). This occurs when Δt is too large, as may occur in models that involve fast voltage clamps or have compartments coupled by very small resistances. However, C-N is safe in most situations, and it can be much more efficient than backward Euler for a given accuracy.

These two methods are almost identical in terms of computational cost per time step (see section 3.3.1). Since the current balance equations have the structure of a tree (there are no current loops), direct gaussian elimination is optimal for their solution (Hines, 1984). This takes exactly the same number of computer operations as would be required for an unbranched cable with the same number of compartments.

The best way to determine the method of choice for any particular problem is to compare both methods with several values of Δt to see which allows the largest Δt consistent with the desired accuracy. In performing such trials, one must remember that the stability properties of a simulation depend on the entire system that is being modeled. Because of interactions between the "biological" components and any "nonbiological" elements, such as stimulators or voltage clamps, the time constants of the entire system may be different from those of the biological components alone. A current source (perfect current clamp) does not affect stability because it does not change the time constants. Any other signal source imposes a load on the compartment to which it is attached, changing the time constants and potentially requiring use of a smaller time step to avoid numerical oscillations in the C-N method. The more closely a signal source approximates a voltage source (perfect voltage clamp), the greater this effect will be.

3.3.1 Efficiency. Nonlinear equations generally need to be solved iteratively to maintain second-order correctness. However, voltage-dependent membrane properties, which are typically formulated in analogy to Hodgkin-Huxley (HH) type channels, allow the cable equation to be cast in a linear form, still second order correct, that can be solved without iterations. A direct solution of the voltage equations at each time step $t \rightarrow t + \Delta t$ using the linearized membrane current $I(V, t) = G \cdot (V - E)$ is sufficient as long as the slope conductance G and the effective reversal potential E are known to second order at time $t + 0.5\Delta t$. HH type channels are easy to solve at $t + 0.5\Delta t$ since the conductance is a function of state variables, which can be computed using a separate time step that is offset by $0.5\Delta t$ with respect to the voltage equation time step. That is, to integrate a state from $t - 0.5\Delta t$ to $t + 0.5\Delta t$, we require only a second-order correct value for the voltage-dependent rates at the midpoint time t.

Figure 5 contrasts this approach with the common technique of replacing nonlinear coefficients by their values at the beginning of a time step. For HH equations in a single compartment, the staggered time grid approach converts four simultaneous nonlinear equations at each time step to four independent linear equations that have the same order of accuracy at each time step. Since the voltage-dependent rates use the voltage at the midpoint of the integration step, integration of channel states can be done analytically in just a single addition and multiplication operation and two table-lookup operations. Although this efficient scheme achieves second-order accuracy,

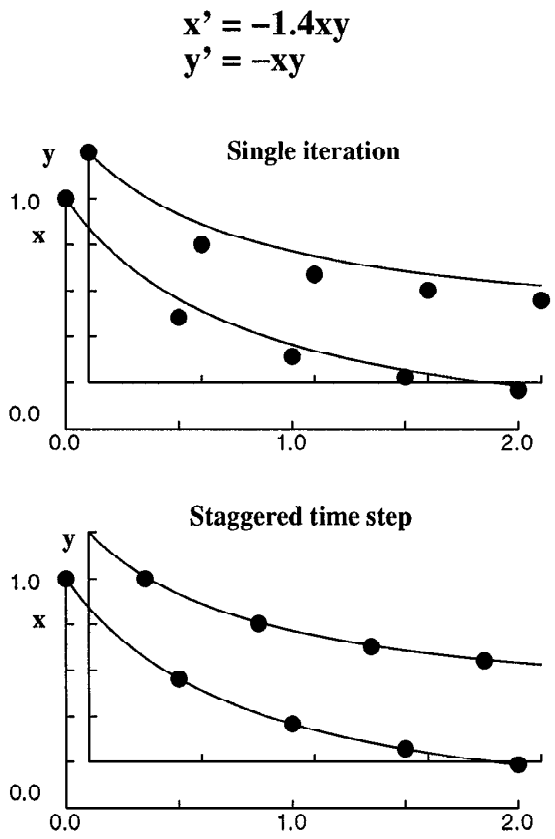

Figure 5: The equations shown at the top of the figure are computed using the Crank-Nicholson method. (Top) $x(t+\Delta t)$ and $y(t+\Delta t)$ are determined using their values at time t. (Bottom) Staggered time steps yield decoupled linear equations. $y(t+\Delta t/2)$ is determined using $x(t)$, after which $x(t+\Delta t)$ is determined using $y(t+\Delta t/2)$.

the trade-off is that the tables depend on the value of the time step and must be recomputed whenever the time step changes.

Neuronal architecture can also be exploited to increase computational efficiency. Since neurons generally have a branched tree structure with no loops, the number of arithmetic operations required to solve the cable equation by gaussian elimination is exactly the same as for an unbranched cable with the same number of compartments. That is, we need only O(N) arith-

metic operations for the equations that describe N compartments connected in the form of a tree, even though standard gaussian elimination generally takes $O(N^3)$ operations to solve N equations in N unknowns. The tremendous efficiency increase results from the fact that in a tree, one can always find a leaf compartment i that is connected to only one other compartment j, so that the equation for compartment i (see equation 3.3a) involves only the voltages in compartments i and j, and the voltage in leaf compartment i is involved only in the equations for compartments i and j (see equations 3.3a and 3.3b):

$$a_{ii}V_i + a_{ij}V_j = b_i \tag{3.3a}$$

$$a_{ji}V_i + a_{jj}V_j + [\text{terms from other compartments}] = b_j. \tag{3.3b}$$

Using equation 3.3a to eliminate the V_i term from equation 3.3b, which requires O(1) (instead of N) operations, gives equation 3.4 and leaves $N-1$ equations in $N-1$ unknowns.

$$a'_{jj}V_j + [\text{terms from other compartments}] = b'_j \tag{3.4}$$

where

$$a'_{jj} = a_{jj} - (a_{ij}a_{ji}/a_{ii})$$

and

$$b'_j = b_j - (b_i a_{ji}/a_{ii}).$$

This strategy can be applied until there is only one equation in one unknown.

Assume that we know the solution to these $N-1$ equations, and in particular that we know V_j. Then we can find V_i from equation 3.3a with O(1) step. Therefore, the effort to solve these N equations is O(1) plus the effort needed to solve $N-1$ equations. The number of operations required is independent of the branching structure, so a tree of N compartments uses exactly the same number of arithmetic operations as a one-dimensional cable of N compartments.

Efficient gaussian elimination requires an ordering that can be found by a simple algorithm: choose the equation with the current minimum number of terms as the equation to use in the elimination step. This minimum degree ordering algorithm is commonly employed in standard sparse matrix solver packages. For example, NEURON's Matrix class uses the matrix library written by Stewart and Leyk (1994). This and many other sparse matrix packages are freely available on the Internet at http://www.netlib.org.

4 The Neuron Simulation Environment

No matter how powerful and robust its computational engine may be, the real utility of any software tool depends largely on its ease of use. Therefore a great deal of effort has been invested in the design of the simulation environment provided by NEURON. In this section we first briefly consider general aspects of the high-level language used for writing NEURON programs. Then we turn to an example of a model of a nerve cell to introduce specific aspects of the user environment, after which we cover these features more thoroughly.

4.1 The hoc Interpreter. NEURON incorporates a programming language based on hoc, a floating-point calculator with C-like syntax described by Kernighan and Pike (1984). This interpreter has been extended by the addition of object-oriented syntax (not including polymorphism or inheritance) that can be used to implement abstract data types and data encapsulation. Other extensions include functions that are specific to the domain of neural simulations and functions that implement a graphical user interface (see below). With hoc one can quickly write short programs that meet most problem-specific needs. The interpreter is used to execute simulations, customize the user interface, optimize parameters, analyze experimental data, calculate new variables such as impulse propagation velocity, and so forth.

NEURON simulations are not subject to the performance penalty often associated with interpreted (as opposed to compiled) languages because computationally intensive tasks are carried out by highly efficient precompiled code. Some of these tasks are related to integration of the cable equation, and others are involved in the emulation of biological mechanisms that generate and regulate chemical and electrical signals.

NEURON provides a built-in implementation of the microemacs text editor. Since the choice of a programming editor is highly personal, NEURON will also accept hoc code in the form of straight ASCII files created with any other editor.

4.2 A Specific Example. In the following example we show how NEURON might be used to model the cell in the top of Figure 6. Comments in the hoc code are preceded by double slashes (//), and code blocks are enclosed in curly brackets ({}).

4.2.1 First Step: Establish Model Topology. One very important feature of NEURON is that it allows the user to think about models in terms that are familiar to the neurophysiologist, keeping numerical issues (e.g., number of spatial segments) entirely separate from the specification of morphology and biophysical properties. This separation is achieved through the use of one-dimensional cable "sections" as the basic building block from which model cells are constructed. These sections can be connected together to

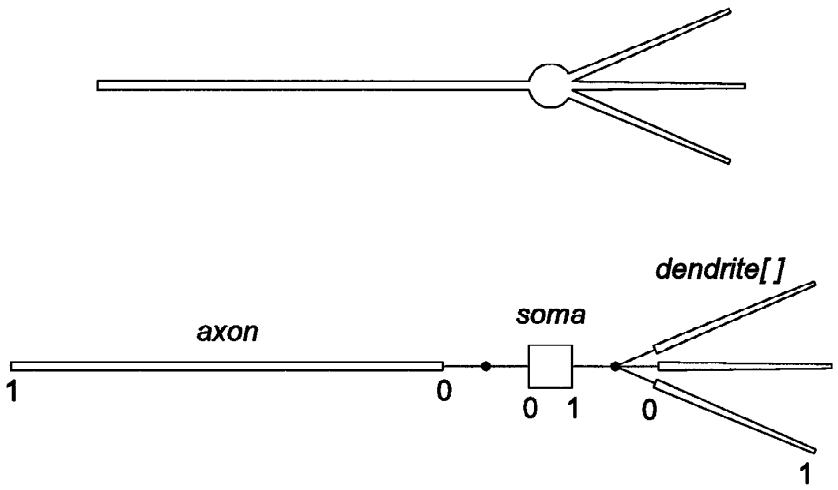

Figure 6: (Top) Cartoon of a neuron with a soma, three dendrites, and an unmyelinated axon (not to scale). The diameter of the spherical soma is 50 μm. Each dendrite is 200 μm long and tapers uniformly along its length from 10 μm diameter at its site of origin on the soma, to 3 μm at its distal end. The unmyelinated cylindrical axon is 1000 μm long and has a diameter of 1 μm. An electrode (not shown) is inserted into the soma for intracellular injection of a stimulating current. (Bottom) Topology of a NEURON model that represents this cell (see text for details).

form any kind of branched cable and endowed with properties that may vary with position along their length.

The idealized neuron in Figure 6 has several anatomical features whose existence and spatial relationships we want the model to include: a cell body (soma), three dendrites, and an unmyelinated axon. The following hoc code sets up the basic topology of the model:

```
create soma, axon, dendrite[3]
connect axon(0), soma(0)
for i=0,2 { connect dendrite[i](0), soma(1) }
```

The program starts by creating named sections that correspond to the important anatomical features of the cell. These sections are attached to each other using `connect` statements. As noted previously, each section has a normalized position parameter `x`, which ranges from 0 at one end to 1 at the other. Because the axon and dendrites arise from opposite sides of the cell body, they are connected to the 0 and 1 ends of the soma section (see the

bottom of Figure 6). A child section can be attached to any location on the parent, but attachment at locations other than 0 or 1 is generally employed only in special cases such as spines on dendrites.

4.2.2 Second Step: Assign Anatomical and Biophysical Properties. Next we set the anatomical and biophysical properties of each section. Each section has its own segmentation, length, and diameter parameters, so it is necessary to indicate which section is being referenced. There are several ways to declare which is the currently accessed section, but here the most convenient is to precede blocks of statements with the appropriate section name:

```
// specify anatomical and biophysical properties
soma {
      nseg = 1          // compartmentalization parameter
      L = 50            // [μm] length
      diam = 50         // [μm] diameter
      insert hh         // standard Hodgkin-Huxley
                        // currents
      gnabar_hh = 0.5*0.120 // max HH sodium conductance
}
axon {
      nseg = 20
      L = 1000
      diam = 1
      insert hh
}
for i=0,2 dendrite[i] {
      nseg = 5
      L = 200
      diam(0:1) = 10:3    // dendritic diameter tapers
                          // along its length
      insert pas          // standard passive current
      e_pas = -65         // [mv] equilibrium potential
                          // for passive current
      g_pas = 0.001       // [siemens/cm^2] conductance
                          // for passive current
}
```

The fineness of the spatial grid is determined by the compartmentalization parameter nseg. Here the soma is lumped into a single compartment (nseg $= 1$), while the axon and each of the dendrites are broken into several subcompartments (nseg $= 20$ and 5, respectively).

In this example, we specify the geometry of each section by assigning values directly to section length and diameter. This creates a stylized model. Alternatively, one can use the 3D method, in which NEURON computes

section length and diameter from a list of (x, y, z, diam) measurements (see section 4.5).

Since the axon is a cylinder, the corresponding section has a fixed diameter along its entire length. The spherical soma is represented by a cylinder with the same surface area as the sphere. The dimensions and electrical properties of the soma are such that its membrane will be nearly isopotential, so the cylinder approximation is not a significant source of error. If chemical signals such as intracellular ion concentrations were important in this model, it would be necessary to approximate not only the surface area but also the volume of the soma.

Unlike the axon, the dendrites become progressively narrower with distance from the soma. Furthermore, unlike the soma, they are too long to be lumped into a single compartment with constant diameter. The taper of the dendrites is accommodated by assigning a sequence of decreasing diameters to their segments. This is done through the use of range variables, which are discussed in section 4.4.

In this model the soma and axon contain HH sodium, potassium, and leak channels (Hodgkin & Huxley, 1952), while the dendrites have constant, linear ("passive") ionic conductances. The `insert` statement assigns the biophysical mechanisms that govern electrical signals in each section. Particular values are set for the density of sodium channels on the soma (`gnabar_hh`) and for the ionic conductance and equilibrium potential of the passive current in the dendrites (`g_pas` and `e_pas`). More information about membrane mechanisms is presented in section 4.6.

4.2.3 Third Step: Attach Stimulating Electrodes. This code emulates the use of an electrode to inject a stimulating current into the soma by placing a current pulse stimulus in the middle of the soma section. The stimulus starts at `t` = 1 ms, lasts for 0.1 ms, and has an amplitude of 60 nA.

```
objref stim
soma stim = new IClamp(0.5)  // put it in middle of soma
stim.del = 1                 // [ms] delay
stim.dur = 0.1               // [ms] duration
stim.amp = 60                // [nA] amplitude
```

The stimulating electrode is an example of a point process. Point processes are discussed in more detail in section 4.6.

4.2.4 Fourth Step: Control Simulation Time Course. At this point all model parameters have been specified. All that remains is to define the simulation parameters, which govern the time course of the simulation, and write some code that executes the simulation.

This is generally done in two procedures. The first procedure initializes the membrane potential and the states of the inserted mechanisms (channel states, ionic concentrations, extracellular potential next to the membrane).

The second procedure repeatedly calls the built-in single-step integration function `fadvance()` and saves, plots, or computes functions of the desired output variables at each step. In this procedure it is possible to change the values of model parameters during a run.

```
dt = 0.05          // [ms] integration time step
tstop = 5          // [ms]
finitialize(-65)   // initialize membrane potential,
                   // state variables, and time

proc integrate() {
     print t, soma.v(0.5)     // show starting time
                              // and initial somatic
                              // membrane potential
     while (t < tstop) {
          fadvance()          // advance solution by dt
          // function calls to save or plot results
          // would go here
          print t, soma.v(0.5)   // show present time
                                 // and somatic
                                 // membrane potential
            // statements that change model parameters
            // would go here
     }
}
```

The built-in function `finitialize()` initializes time `t` to 0, membrane potential `v` to -65 mv throughout the model, and the HH state variables *m*, *n*, and *h* to their steady-state values at `v` $= -65$ mv. Initialization can also be performed with a user-written routine if there are special requirements that `finitialize()` cannot accommodate, such as nonuniform membrane potential.

Both the integration time step `dt` and the solution time `t` are global variables. For this example `dt` = 50 μs. The `while(){}` statement repeatedly calls `fadvance()`, which integrates the model equations over the interval `dt` and increments `t` by `dt` on each call. For this example, the time and somatic membrane potential are displayed at each step. This loop exits when `t` $\geq$ `tstop`.

When this program is first processed by the NEURON interpreter, the model is set up and initiated, but the `integrate()` procedure is not executed. When the user enters an `integrate()` statement in the NEURON interpreter window, the simulation advances for 5 ms using 50 μs time steps.

4.3 Section Variables. Three parameters apply to the section as a whole: cytoplasmic resistivity `Ra` (Ω cm), the section length `L`, and the compartmentalization parameter `nseg`. The first two are ordinary in the sense that they

do not affect the structure of the equations that describe the model. Note that the hoc code specifies values for L but not for Ra. This is because each section in a model is likely to have a different length, whereas the cytoplasm (and therefore Ra) is usually assumed to be uniform throughout the cell. The default value of Ra is 35.4 Ω cm, which is appropriate for invertebrate neurons. Like L it can be assigned a new value in any or all sections (e.g., ~200 Ω cm for mammalian neurons).

The user can change the compartmentalization parameter nseg without having to modify any of the statements that set anatomical or biophysical properties. However, if parameters vary with position in a section, care must be taken to ensure that the model incorporates the spatial detail inherent in the parameter description.

4.4 Range Variables. Like dendritic diameter in our example, most cellular properties are functions of the position parameter x. NEURON has special provisions for dealing with these properties, which are called range variables. Other examples of range variables are the membrane potential v and ionic conductance parameters such as the maximum HH sodium conductance gnabar_hh (siemens / cm^2).

Range variables enable the user to separate property specification from segment number. A range variable is assigned a value in one of two ways. The simpler and more common is as a constant. For example, the statement axon.diam = 10 asserts that the diameter of the axon is uniform over its entire length.

The syntax for a property that changes along a length of a section is rangevar(*xmin* : *xmax*) = *e*1 : *e*2. The four italicized symbols are expressions, with *e*1 and *e*2 being the values of the property at *xmin* and *xmax*, respectively. The position expressions must meet the constraint $0 \leq xmin \leq xmax \leq 1$. Linear interpolation is used to assign the values of the property at the segment centers that lie in the position range [*xmin*, *xmax*]. In this manner a continuously varying property can be approximated by a piecewise linear function. If the range variable is diameter, neither *e*1 nor *e*2 should be 0, or corresponding axial resistance will be infinite.

In our model neuron, the simple dendritic taper is specified by diam(0:1) = 10:3 and nseg = 5. This results in five segments that have centers at x = 0.1, 0.3, 0.5, 0.7, and 0.9 and diameters of 9.3, 7.9, 6.5, 5.1, and 3.7, respectively.

The value of a range variable at the center of a segment can appear in any expression using the syntax rangevar(x) in which $0 \leq x \leq 1$. The value returned is the value at the center of the segment containing x, not the linear interpolation of the values stored at the centers of adjacent segments. If the parentheses are omitted, the position defaults to a value of 0.5 (middle of the section).

A special form of the for statement is available: for (var) stmt. For each value of the normalized position parameter x that defines the center

of each segment in the selected section (along with positions 0 and 1), this statement assigns `var` that value and executes the `stmt`. This `hoc` code would print the membrane potential as a function of physical position (in μm) along the axon:

```
axon for (x) print x*L, v(x)
```

4.5 Specifying Geometry: Stylized versus 3D. There are two ways to specify section geometry. Our example uses the stylized method, which simply assigns values to section length and diameter. This is most appropriate when cable length and diameter are authoritative and 3D shape is irrelevant.

If the model is based on anatomical reconstruction data (quantitative morphometry) or if 3D visualization is paramount, it is better to use the 3D method. This approach keeps the anatomical data in a list of (x, y, z, diam) "points." The first point is associated with the end of the section that is connected to the parent (this is not necessarily the zero end), and the last point is associated with the opposite end. There must be at least two points per section, and they should be ordered in terms of monotonically increasing arc length. This pt3d list, which is the authoritative definition of the shape of the section, automatically determines the length and diameter of the section.

When the pt3d list is nonempty, the shape model used for a section is a sequence of frusta. The pt3d points define the locations and diameters of the ends of these frusta. The effective area, diameter, and resistance of each segment are computed from this sequence of points by trapezoidal integration along the segment length. This takes into account the extra area introduced by diameter changes; even degenerate cones of 0 length can be specified (i.e., two points with same coordinates but different diameters), which add area but not length to the section. No attempt is made to deal with the effects of centroid curvature on surface area. The number of 3D points used to describe a shape has nothing to do with `nseg` and does not affect simulation speed.

4.6 Density Mechanisms and Point Processes. The `insert` statement assigns biophysical mechanisms, which govern electrical and (if present) chemical signals, to a section. Many sources of electrical and chemical signals are distributed over the membrane of the cell. These density mechanisms are described in terms of current per unit area and conductance per unit area; examples include voltage-gated ion channels such as the HH currents. However, density mechanisms are not the most appropriate representation of all signal sources. Synapses and electrodes are best described in terms of localized absolute current in nanoamperes and conductance in microsiemens. These are called point processes.

An object syntax is used to manage the creation, insertion, attributes, and destruction of point processes. For example, a current clamp (electrode for injecting a current) is created by declaring an object variable and assigning it a new instance of the IClamp object class. When a point process is no longer referenced by any object variable, the point process is removed from the section and destroyed. In our example, redeclaring `stim` with the statement `objref stim` would destroy the pulse stimulus, since no other object variable is referencing it.

The location of a point process can be changed with no effect on its other attributes. In our example, the statement `dendrite[2] stim.loc(1)` would move the current stimulus to the distal end of the third dendrite.

Many user-defined density mechanisms and point processes can be simultaneously present in each compartment of a neuron. One important difference between density mechanisms and point processes is that any number of the same kind of point process can exist at the same location.

User-defined density mechanisms and point processes can be linked into NEURON using the model description language NMODL. This lets the user focus on specifying the equations for a channel or ionic process without regard to its interactions with other mechanisms. The NMODL translator then constructs the appropriate C program, which is compiled and becomes available for use in NEURON. This program properly and efficiently computes the total current of each ionic species used, as well as the effect of that current on ionic concentration, reversal potential, and membrane potential. An extensive discussion of NMODL is beyond the scope of this article, but its major advantages can be listed succinctly.

1. Interface details to NEURON are handled automatically, and there are a great many such details. NEURON needs to know that model states are range variables and which model parameters can be assigned values and evaluated from the interpreter. Point processes need to be accessible via the interpreter object syntax, and density mechanisms need to be added to a section when the “insert” statement is executed. If two or more channels use the same ion at the same place, the individual current contributions need to be added together to calculate a total ionic current.
2. Consistency of units is ensured.
3. Mechanisms described by kinetic schemes are written with a syntax in which the reactions are clearly apparent. The translator provides tremendous leverage by generating a large block of C code that calculates the analytic Jacobian and the state fluxes.
4. There is often a great increase in clarity since statements are at the model level instead of the C programming level and are independent of the numerical method. For example, sets of differential and non-

linear simultaneous equations are written using an expression syntax such as

```
x' = f(x, y, t)
~ g(x, y) = h(x, y)
```

where the prime refers to the derivative with respect to time (multiple primes such as `x''` refer to higher derivatives), and the tilde introduces an algebraic equation. The algebraic portion of such systems of equations is solved by Newton's method, and a variety of methods are available for solving the differential equations, such as Runge-Kutta or backward Euler.

5. Function tables can be generated automatically for efficient computation of complicated expressions.
6. Default initialization behavior of a channel can be specified.

4.7 Graphical Interface. The user is not limited to operating within the traditional code-based command-mode environment. Among its many extensions to hoc, NEURON includes functions for implementing a fully graphical, windowed interface. Through this interface, and without having to write any code at all, the user can effortlessly create and arrange displays of menus, parameter value editors, graphs of parameters and state variables, and views of the model neuron. Anatomical views, called space plots, can be explored, revealing what mechanisms and point processes are present and where they are located.

The purpose of NEURON's graphical interface is to promote a match between what the user thinks is inside the computer and what is actually there. These visualization enhancements are a major aid to maintaining conceptual control over the simulation because they provide immediate answers to questions about what is being represented in the computer.

The interface has no provision for constructing neuronal topology, a conscious design choice based on the strong likelihood that a graphical toolbox for building neuronal topologies would find little use. Small models with simple topology are so easily created in hoc that a graphical topology editor is unnecessary. More complex models are too cumbersome to deal with using a graphical editor. It is best to express the topological specifications of complex stereotyped models through algorithms, written in hoc, that generate the topology automatically. Biologically realistic models often involve hundreds or thousands of sections, whose dimensions and interconnections are contained in large data tables generated by hours of painstaking quantitative morphometry. These tables are commonly read by hoc procedures that in turn create and connect the required sections without operator intervention.

The basic features of the graphical interface and how to use it to monitor and control simulations are discussed elsewhere (Moore & Hines, 1996).

However, several sophisticated analysis and simulation tools that have special utility for nerve simulation are worthy of mention:

- The Function Fitter optimizes a parameterized mathematical expression to minimize the least squared difference between the expression and data.
- The Run Fitter allows one to optimize several parameters of a complete neuron model to experimental data. This is most useful in the context of voltage clamp data that are contaminated by incomplete space clamp or models that cannot be expressed in closed form, such as kinetic schemes for channel conductance.
- The Electrotonic Workbench plots small signal input and transfer impedance and voltage attenuation as functions of space and frequency (Carnevale, Tsai, & Hines, 1996). These plots include the neuromorphic (Carnevale, Tsai, Claiborne, & Brown, 1995) and L versus x (O'Boyle, Barrevale, Carnevale, Claiborne, & Brown, 1996) renderings of the electrotonic transformation (Brown et al., 1992; Tsai, Carnevale, Claiborne, & Brown, 1994; Zador, Agmon-Snir, & Segev, 1995). By revealing the effectiveness of signal transfer, the Workbench quickly provides insight into the "functional shape" of a neuron.

All interactions with these and other tools takes place in the graphical interface, and no interpreter programming is needed to use them. However, they are constructed entirely within the interpreter and can be modified when special needs require.

4.8 Object-Oriented Syntax.

4.8.1 Neurons. It is often convenient to deal with groups of sections that are related. Therefore NEURON provides a data class called a `SectionList` that can be used to identify subsets of sections. Section lists fit nicely with the "regular expression" method of selecting sections, used in earlier implementations of NEURON, in that the section list is easily constructed by using regular expressions to add and delete sections. After the list is constructed it is available for reuse, and it is much more efficient to loop over the sections in a section list than to pick out the sections accepted by a combination of regular expressions. This code

```
objref alldend
alldend = new SectionList()
forsec "dend" alldend.append()
forsec alldend print secname()
```

forms a list of all the sections whose names contain the string "dend" and then iterates over the list, printing the name of each section in it. For the example program presented here, this would generate the following output

in the NEURON interpreter window,

```
dendrite[0]
dendrite[1]
dendrite[2]
```

although in this very simple example it would clearly have been easy enough to loop over the array of dendrites directly, for example:

```
for i = 0,2 {
     dendrite[i] print secname()
}
```

4.8.2 Networks. To help the user manage very large simulations, the interpreter syntax has been extended to facilitate the construction of hierarchical objects. This is illustrated by the following code fragment, which specifies a pattern for a simple stylized neuron consisting of three dendrites connected to one end of a soma and an axon connected to the other end:

```
begintemplate Cell1
      public soma, dendrite, axon
      create soma, dendrite[3], axon
      proc init() {
             for i=0,2 connect dendrite[i](0), soma(0)
             connect axon(0), soma(1)
             axon insert hh
   }
endtemplate Cell1
```

Whenever a new instance of this pattern is created, the `init()` procedure automatically connects the `soma`, `dendrite`, and `axon` sections together. A complete pattern would also specify default membrane properties, as well as the number of segments for each section.

Names that can be referenced outside the pattern are listed in the `public` statement. In this case, since `init` is not in the list, the user could not reinitialize by calling the `init()` procedure. Public names are referenced through a dot notation.

The particular benefit of using templates ("classes" in standard object-oriented terminology) is the fact that they can be employed to create any number of instances of a pattern. For example,

```
objref cell[10][10]
for i=0,9 for j=0,9 cell[i][j]=new Cell1()
```

creates an array of one hundred objects of type `Cell1` that can be referenced individually by the object variable `cell`. In this example, `cell[4][5].axon. gnabar_hh(0.5)` is the value of the maximum HH sodium conductance in the middle of the axon of `cell[4][5]`.

As this example implies, templates offer a natural syntax for the creation of networks. However, it is entirely up to the user to organize the templates logically so that they appropriately reflect the structure of the problem. Generally any given structural organization can be viewed as a hierarchy of container classes, such as cells, microcircuits, layers, or networks. The important issue is how much effort is required for the concrete network representation to support a range of logical views of the same abstract network. A logical view that organizes the cells differently may not be easy to compute if the network is built as an elaborate hierarchy. This kind of pressure tends to encourage relatively flat organizations that make it easier to implement functions that search for specific information. The bottom line is that network simulation design remains an ad hoc process that requires careful programming judgment.

One very important class of logical views that are not generally organizable as a hierarchy are those of synaptic organization. In connecting cells with synapses, one is often driven to deal with general graphs, which is to say no structure at all.

In addition to the notions of classes and objects (a synapse is an object with a pre- and a postsynaptic logical connection) the interpreter offers one other fundamental language feature that can be useful in dealing with objects that are collections of other objects: the notion of iterators, taken from the Sather programming language (Murer, Omohundro, Stoutamire, & Szyerski, 1996). This is a separation of the process of iteration from that of "what is to be done for each item." If a programmer implements one or more iterators in a collection class, the user of the class does not need to know how the class indexes its items. Instead the class will return each item in turn for execution in the context of the loop body. This allows the user to write

```
for layer1.synapses(syn, type) {
    // statements that manipulate the object
    // reference named "syn" (The iterator
    // causes "syn" to refer, in turn, to
    // each synapse of a certain type in
    // the layer1 object)
}
```

without being aware of the possibly complicated process of picking out these synapses from the layer (that is the responsibility of the author of the class of which `layer1` is an instance).

It is to be sadly emphasized that these kinds of language features, though very useful, do not impose any policy with regard to the design decisions that users must make in building their networks. Different programmers express very different designs on the same language base, with the consequence that it is more often than not infeasible to reconcile slightly different representations of even very similar concepts.

An example of a useful way to deal uniformly with the issue of synaptic connectivity is the policy implemented in NEURON by Lytton (1996). This implementation uses the normal NMODL methodology to define a synaptic conductance model and enclose it within a framework that manages network connectivity.

5 Summary

The recent striking expansion in the use of simulation tools in the field of neuroscience has been encouraged by the rapid growth of quantitative observations that both stimulate and constrain the formulation of new hypotheses of neuronal function, enabled by the availability of ever-increasing computational power at low cost. These factors have motivated the design and implementation of NEURON, the goal of which is to provide a powerful and flexible environment for simulations of individual neurons and networks of neurons. NEURON has special features that accommodate the complex geometry and nonlinearities of biologically realistic models, without interfering with its ability to handle more speculative models that involve a high degree of abstraction.

As we note in this article, one particularly advantageous feature is that the user can specify the physical properties of a cell without regard for the strictly computational concern of how many compartments are employed to represent each of the cable sections. In a future publication, we will examine how the NMODL translator is used to define new membrane channels and calculate ionic concentration changes. Another will describe the Vector class. In addition to providing very efficient implementations of frequently needed operations on lists of numbers, the vector class offers a great deal of programming leverage, especially in the management of network models.

NEURON source code, executables, and documents are available at http://neuron.duke.edu and http://www.neuron.yale.edu, and by ftp from ftp.neuron.yale.edu.

Acknowledgments

We thank John Moore, Zach Mainen, Bill Lytton, David Jaffe, and the many other users of NEURON for their encouragement, helpful suggestions, and other contributions. This work was supported by NIH grant NS 11613 (Computer Methods for Physiological Problems) to M.L.H. and by the Yale Neuroengineering and Neuroscience Center.

References

Bernander, O., Douglas, R. J., Martin, K. A. C., & Koch, C. (1991). Synaptic background activity influences spatiotemporal integration in single pyramidal cells. *Proc. Nat. Acad. Sci., 88,* 11569–11573.

Brown, T. H., Zador, A. M., Mainen, Z. F., & Claiborne, B. J. (1992). Hebbian computations in hippocampal dendrites and spines. In T. McKenna, J. Davis, & S. F. Zornetzer (Eds.), *Single Neuron Computation* (pp. 81–116). San Diego: Academic Press.

Carnevale, N. T., & Rosenthal, S. (1992). Kinetics of diffusion in a spherical cell: I. No solute buffering. *J. Neurosci. Meth., 41*, 205–216.

Carnevale, N. T., Tsai, K. Y., Claiborne, B. J., & Brown, T. H. (1995). The electrotonic transformation: A tool for relating neuronal form to function. In G. Tesauro, D. S. Touretzky, & T. K. Leen (Eds.), *Advances in Neural Information Processing Systems* (vol. 7, pp. 69–76). Cambridge, MA: MIT Press.

Carnevale, N. T., Tsai, K. Y., & Hines, M. L. (1996). The Electrotonic Workbench. *Society for Neuroscience Abstracts, 22*, 1741.

Cauller, L. J., & Connors, B. W. (1992). Functions of very distal dendrites: Experimental and computational studies of layer I synapses on neocortical pyramidal cells. In T. McKenna, J. Davis, & S. F. Zornetzer (Eds.), *Single Neuron Computation* (pp. 199–229). San Diego: Academic Press.

Destexhe, A., Babloyantz, A., & Sejnowski, T. J. (1993). Ionic mechanisms for intrinsic slow oscillations in thalamic relay neurons. *Biophys. J., 65*, 1538–1552.

Destexhe, A., Contreras, D., Sejnowski, T. J., & Steriade, M. (1994). A model of spindle rhythmicity in the isolated thalamic reticular nucleus. *J. Neurophysiol., 72*, 803–818.

Destexhe, A., Contreras, D., Steriade, M., Sejnowski, T. J., & Huguenard, J. R. (1996). In vivo, in vitro and computational analysis of dendritic calcium currents in thalamic reticular neurons. *J. Neurosci., 16*, 169–185.

Destexhe, A., McCormick, D. A., & Sejnowski, T. J. (1993). A model for 8–10 Hz spindling in interconnected thalamic relay and reticularis neurons. *Biophys. J., 65*, 2474–2478.

Destexhe, A., & Sejnowski, T. J. (1995). G-protein activation kinetics and spillover of GABA may account for differences between inhibitory responses in the hippocampus and thalamus. *Proc. Nat. Acad. Sci., 92*, 9515–9519.

Häusser, M., Stuart, G., Racca, C., & Sakmann, B. (1995). Axonal initiation and active dendritic propagation of action potentials in substantia nigra neurons. *Neuron, 15*, 637–647.

Hines, M. (1984). Efficient computation of branched nerve equations. *Int. J. Bio-Med. Comput., 15*, 69–76.

Hines, M. (1989). A program for simulation of nerve equations with branching geometries. *Int. J. Bio-Med. Comput., 24*, 55–68.

Hines, M. (1993). NEURON—a program for simulation of nerve equations. In F. Eeckman (Ed.), *Neural Systems: Analysis and Modeling* (pp. 127–136). Norwell, MA: Kluwer.

Hines, M. (1994). The NEURON simulation program. In J. Skrzypek (Ed.), *Neural Network Simulation Environments* (pp. 147–163). Norwell, MA: Kluwer.

Hines, M., & Carnevale, N. T. (1995). Computer modeling methods for neurons. In M. A. Arbib (Ed.), *The Handbook of Brain Theory and Neural Networks* (pp. 226–230). Cambridge, MA: MIT Press.

Hines, M., & Shrager, P. (1991). A computational test of the requirements for conduction in demyelinated axons. *J. Restor. Neurol. Neurosci., 3*, 81–93.

Hodgkin, A. L., & Huxley, A. F. (1952). A quantitative description of membrane current and its application to conduction and excitation in nerve. *J. Physiol., 117*, 500–544.

Hsu, H., Huang, E., Yang, X.-C., Karschin, A., Labarca, C., Figl, A., Ho, B., Davidson, N., & Lester, H. A. (1993). Slow and incomplete inactivations of voltage-gated channels dominate encoding in synthetic neurons. *Biophys. J., 65*, 1196–1206.

Jaffe, D. B., Ross, W. N., Lisman, J. E., Miyakawa, H., Lasser-Ross, N., & Johnston, D. (1994). A model of dendritic Ca2+ accumulation in hippocampal pyramidal neurons based on fluorescence imaging experiments. *J. Neurophysiol., 71*, 1065–1077.

Kernighan, B. W., & Pike, R. (1984). Appendix 2: Hoc manual. In B. W. Kernighen & R. Pike (Eds.), *The UNIX Programming Environment* (pp. 329–333). Englewood Cliffs, NJ: Prentice Hall.

Lindgren, C. A., & Moore, J. W. (1989). Identification of ionic currents at presynaptic nerve endings of the lizard. *J. Physiol., 414*, 210–222.

Lytton, W. W. (1996). Optimizing synaptic conductance calculation for network simulations. *Neural Computation, 8*, 501–509.

Lytton, W. W., Destexhe, A., & Sejnowski, T. J. (1996). Control of slow oscillations in the thalamocortical neuron: A computer model. *Neurosci., 70*, 673–684.

Lytton, W. W., & Sejnowski, T. J. (1992). Computer model of ethosuximide's effect on a thalamic neuron. *Ann. Neurol., 32*, 131–139.

Mainen, Z. F., Joerges, J., Huguenard, J., & Sejnowski, T. J. (1995). A model of spike initiation in neocortical pyramidal neurons. *Neuron, 15*, 1427–1439.

Mainen, Z. F., & Sejnowski, T. J. (1995). Reliability of spike timing in neocortical neurons. *Science, 268*, 1503–1506.

Mascagni, M. V. (1989). Numerical methods for neuronal modeling. In C. Koch & I. Segev (Eds.), *Methods in Neuronal Modeling* (pp. 439–484). Cambridge, MA: MIT Press.

Moore, J. W., & Hines, M. (1996). Simulations with NEURON 3.1, on-line documentation in HTML format, available at http://neuron.duke.edu.

Murer, S., Omohundro, S. M., Stoutamire, D., & Szyerski, C. (1996). Iteration abstraction in Sather. *ACM Transactions on Programming Languages and Systems, 18*, 1–15.

O'Boyle, M. P., Carnevale, N. T., Claiborne, B. J., & Brown, T. H. (1996). A new graphical approach for visualizing the relationship between anatomical and electrotonic structure. In J. M. Bower (Ed.), *Computational Neuroscience: Trends in Research 1995*. San Diego: Academic Press.

Rall, W. (1964). Theoretical significance of dendritic tree for input-output relation. In R. F. Reiss (Ed.), *Neural Theory and Modeling* (pp. 73–97). Stanford: Stanford University Press.

Rall, W. (1989). Cable theory for dendritic neurons. In C. Koch & I. Segev (Ed.), *Methods in Neuronal Modeling* (pp. 8–62). Cambridge, MA: MIT Press.

Softky, W. (1994). Sub-millisecond coincidence detection in active dendritic trees. *Neurosci., 58*, 13–41.

Stewart, D., & Leyk, Z. (1994). Meschach: Matrix computations in C. In *Proceedings of the Centre for Mathematics and Its Applications* (Vol. 32). Canberra, Australia: School of Mathematical Sciences, Australian National University.

Traynelis, S. F., Silver, R. A., & Cull-Candy, S. G. (1993). Estimated conductance of glutamate receptor channels activated during epscs at the cerebellar mossy fiber-granule cell synapse. *Neuron, 11*, 279–289.

Tsai, K. Y., Carnevale, N. T., & Brown, T. H. (1994). Hebbian learning is jointly controlled by electrotonic and input structure. *Network, 5*, 1–19.

Tsai, K. Y., Carnevale, N. T., Claiborne, B. J., & Brown, T. H. (1994). Efficient mapping from neuroanatomical to electrotonic space. *Network, 5*, 21–46.

Zador, A. M., Agmon-Snir, H., & Segev, I. (1995). The morphoelectrotonic transform: A graphical approach to dendritic function. *J. Neurosci., 15*, 1669–1682.

Received September 26, 1996; accepted January 10, 1997.

This article has been cited by:

1. Tyler P. Lee, Dean V. Buonomano. 2012. Unsupervised Formation of Vocalization-Sensitive Neurons: A Cortical Model Based on Short-Term and Homeostatic Plasticity. *Neural Computation* **24**:10, 2579-2603. [Abstract] [Full Text] [PDF] [PDF Plus] [Supplementary Content]
2. Palmi Thor Thorbergsson, Martin Garwicz, Jens Schouenborg, Anders J Johansson. 2012. Computationally efficient simulation of extracellular recordings with multielectrode arrays. *Journal of Neuroscience Methods* **211**:1, 133-144. [CrossRef]
3. J.S. Cruz, C. Kushmerick, D.C. Moreira-Lobo, F.A. Oliveira. 2012. Thiamine deficiency in vitro accelerates A-type potassium current inactivation in cerebellar granule neurons. *Neuroscience* **221**, 108-114. [CrossRef]
4. Claude Bédard, Sebastien Béhuret, Charlotte Deleuze, Thierry Bal, Alain Destexhe. 2012. Oversampling method to extract excitatory and inhibitory conductances from single-trial membrane potential recordings. *Journal of Neuroscience Methods* **210**:1, 3-14. [CrossRef]
5. Hyun Jae Jang, Jeehyun Kwag. 2012. GABAA receptor-mediated feedforward and feedback inhibition differentially modulates hippocampal spike timing-dependent plasticity. *Biochemical and Biophysical Research Communications* . [CrossRef]
6. Sébastien Joucla, Lionel Rousseau, Blaise Yvert. 2012. Focalizing electrical neural stimulation with penetrating microelectrode arrays: A modeling study. *Journal of Neuroscience Methods* **209**:1, 250-254. [CrossRef]
7. Marcus E. Petersson, Erik Fransén. 2012. Long-lasting small-amplitude TRP-mediated dendritic depolarizations in CA1 pyramidal neurons are intrinsically stable and originate from distal tuft regions. *European Journal of Neuroscience* no-no. [CrossRef]
8. Ashutosh Chaturvedi, Thomas J. Foutz, Cameron C. McIntyre. 2012. Current steering to activate targeted neural pathways during deep brain stimulation of the subthalamic region. *Brain Stimulation* **5**:3, 369-377. [CrossRef]
9. Izumi Fukunaga, Manuel Berning, Mihaly Kollo, Anja Schmaltz, Andreas T. Schaefer. 2012. Two Distinct Channels of Olfactory Bulb Output. *Neuron* **75**:2, 320-329. [CrossRef]
10. Patrick Crotty, Eric Lasker, Sen Cheng. 2012. Constraints on the synchronization of entorhinal cortex stellate cells. *Physical Review E* **86**:1. . [CrossRef]
11. Albert Gidon, Idan Segev. 2012. Principles Governing the Operation of Synaptic Inhibition in Dendrites. *Neuron* **75**:2, 330-341. [CrossRef]
12. T. Dugladze, D. Schmitz, M. A. Whittington, I. Vida, T. Gloveli. 2012. Segregation of Axonal and Somatic Activity During Fast Network Oscillations. *Science* **336**:6087, 1458-1461. [CrossRef]
13. Michelle Rudolph-Lilith, Mathieu Dubois, Alain Destexhe. 2012. Analytical Integrate-and-Fire Neuron Models with Conductance-Based Dynamics and Realistic Postsynaptic Potential Time Course for Event-Driven Simulation Strategies. *Neural Computation* **24**:6, 1426-1461. [Abstract] [Full Text] [PDF] [PDF Plus]
14. Huifang Ji, Kristal R. Tucker, Ilva Putzier, Marco A. Huertas, John P. Horn, Carmen C. Canavier, Edwin S. Levitan, Paul D. Shepard. 2012. Functional characterization of ether-à-go-go-related gene potassium channels in midbrain dopamine neurons - implications for a role in depolarization block. *European Journal of Neuroscience* no-no. [CrossRef]
15. Roy Ben-Shalom, Amit Aviv, Benjamin Razon, Alon Korngreen. 2012. Optimizing ion channel models using a parallel genetic algorithm on graphical processors. *Journal of Neuroscience Methods* **206**:2, 183-194. [CrossRef]
16. Athan Spiros, Patrick Roberts, Hugo Geerts. 2012. A Quantitative Systems Pharmacology Computer Model for Schizophrenia Efficacy and Extrapyramidal Side Effects. *Drug Development Research* n/a-n/a. [CrossRef]
17. Sébastien Joucla, Blaise Yvert. 2012. Modeling extracellular electrical neural stimulation: From basic understanding to MEA-based applications. *Journal of Physiology-Paris* **106**:3-4, 146-158. [CrossRef]
18. Keivan Moradi, Gholamreza Kaka, Shahriar Gharibzadeh. 2012. The role of passive normalization, voltage-gated channels and synaptic scaling in site-independence of somatic EPSP amplitude in CA1 pyramidal neurons. *Neuroscience Research* **73**:1, 8-16. [CrossRef]
19. R. Sittl, A. Lampert, T. Huth, E. T. Schuy, A. S. Link, J. Fleckenstein, C. Alzheimer, P. Grafe, R. W. Carr. 2012. Anticancer drug oxaliplatin induces acute cooling-aggravated neuropathy via sodium channel subtype NaV1.6-resurgent and persistent current. *Proceedings of the National Academy of Sciences* . [CrossRef]

20. Hiroshi Kameda, Hiroyuki Hioki, Yasuyo H. Tanaka, Takuma Tanaka, Jaerin Sohn, Takahiro Sonomura, Takahiro Furuta, Fumino Fujiyama, Takeshi Kaneko. 2012. Parvalbumin-producing cortical interneurons receive inhibitory inputs on proximal portions and cortical excitatory inputs on distal dendrites. *European Journal of Neuroscience* **35**:6, 838-854. [CrossRef]
21. Therese Abrahamsson, Laurence Cathala, Ko Matsui, Ryuichi Shigemoto, David A. DiGregorio. 2012. Thin Dendrites of Cerebellar Interneurons Confer Sublinear Synaptic Integration and a Gradient of Short-Term Plasticity. *Neuron* **73**:6, 1159-1172. [CrossRef]
22. Winfried Denk, Kevin L. Briggman, Moritz Helmstaedter. 2012. Structural neurobiology: missing link to a mechanistic understanding of neural computation. *Nature Reviews Neuroscience* . [CrossRef]
23. Manuel Marx, Robert H Günter, Werner Hucko, Gabriele Radnikow, Dirk Feldmeyer. 2012. Improved biocytin labeling and neuronal 3D reconstruction. *Nature Protocols* **7**:2, 394-407. [CrossRef]
24. Mark S. Cembrowski, Stephen M. Logan, Miao Tian, Li Jia, Wei Li, William L. Kath, Hermann Riecke, Joshua H. Singer. 2012. The Mechanisms of Repetitive Spike Generation in an Axonless Retinal Interneuron. *Cell Reports* **1**:2, 155-166. [CrossRef]
25. Sergey M. Korogod, Anton V. Kaspirzhny. 2012. Spatial heterogeneity of passive electrical transfer properties of neuronal dendrites due to their metrical asymmetry. *Biological Cybernetics* . [CrossRef]
26. Daniel Jungblut, Andreas Vlachos, Gerlind Schuldt, Nadine Zahn, Thomas Deller, Gabriel Wittum. 2012. SpineLab: tool for three-dimensional reconstruction of neuronal cell morphology. *Journal of Biomedical Optics* **17**:7, 076007. [CrossRef]
27. Le Wang, H. Steven Colburn. 2011. A Modeling Study of the Responses of the Lateral Superior Olive to Ipsilateral Sinusoidally Amplitude-Modulated Tones. *Journal of the Association for Research in Otolaryngology* . [CrossRef]
28. Jian K. Liu. 2011. Learning Rule of Homeostatic Synaptic Scaling: Presynaptic Dependent or Not. *Neural Computation* **23**:12, 3145-3161. [Abstract] [Full Text] [PDF] [PDF Plus] [Supplementary Content]
29. S. Ramaswamy, S. L. Hill, J. G. King, F. Schurmann, Y. Wang, H. Markram. 2011. Intrinsic Morphological Diversity of Thick-tufted Layer 5 Pyramidal Neurons Ensures Robust and Invariant Properties of in silico Synaptic Connections. *The Journal of Physiology* . [CrossRef]
30. Sharmila Venugopal, Sharon Crook, Malathi Srivatsan, Ranu JungPrinciples of Computational Neuroscience 11-30. [CrossRef]
31. Martin Pospischil, Zuzanna Piwkowska, Thierry Bal, Alain Destexhe. 2011. Comparison of different neuron models to conductance-based post-stimulus time histograms obtained in cortical pyramidal cells using dynamic-clamp in vitro. *Biological Cybernetics* . [CrossRef]
32. Emre Neftci, Elisabetta Chicca, Giacomo Indiveri, Rodney Douglas. 2011. A Systematic Method for Configuring VLSI Networks of Spiking Neurons. *Neural Computation* **23**:10, 2457-2497. [Abstract] [Full Text] [PDF] [PDF Plus]
33. Jenny Tigerholm, Erik Fransén. 2011. Reversing Nerve Cell Pathology by Optimizing Modulatory Action on Target Ion Channels. *Biophysical Journal* **101**:8, 1871-1879. [CrossRef]
34. Alexis M. Kuncel, Merrill J. Birdno, Brandon D. Swan, Warren M. Grill. 2011. Tremor reduction and modeled neural activity during cycling thalamic deep brain stimulation. *Clinical Neurophysiology* . [CrossRef]
35. W.L. Nowinski, B.C. Chua, G.Y. Qian, N.G. Nowinska. 2011. The human brain in 1700 pieces: Design and development of a three-dimensional, interactive and reference atlas. *Journal of Neuroscience Methods* . [CrossRef]
36. D Michael Ackermann, Niloy Bhadra, Meana Gerges, Peter J Thomas. 2011. Dynamics and sensitivity analysis of high-frequency conduction block. *Journal of Neural Engineering* **8**:6, 065007. [CrossRef]
37. Yoshiyuki Kubota, Fuyuki Karube, Masaki Nomura, Allan T. Gulledge, Atsushi Mochizuki, Andreas Schertel, Yasuo Kawaguchi. 2011. Conserved properties of dendritic trees in four cortical interneuron subtypes. *Scientific Reports* **1**. . [CrossRef]
38. Xiumin Li, Kenji Morita, Hugh P. C. Robinson, Michael Small. 2011. Impact of gamma-oscillatory inhibition on the signal transmission of a cortical pyramidal neuron. *Cognitive Neurodynamics* . [CrossRef]
39. Michele Migliore, Ignazio De Blasi, Domenico Tegolo, Rosanna Migliore. 2011. A modeling study suggesting how a reduction in the context-dependent input on CA1 pyramidal neurons could generate schizophrenic behavior. *Neural Networks* **24**:6, 552-559. [CrossRef]
40. Scott F Lempka, Matthew D Johnson, Michael A Moffitt, Kevin J Otto, Daryl R Kipke, Cameron C McIntyre. 2011. Theoretical analysis of intracortical microelectrode recordings. *Journal of Neural Engineering* **8**:4, 045006. [CrossRef]
41. Harilal Parasuram, Bipin Nair, Giovanni Naldi, Egidio D'Angelo, Shyam Diwakar. 2011. A modeling based study on the origin and nature of evoked post-synaptic local field potentials in granular layer. *Journal of Physiology-Paris* . [CrossRef]

42. John Eric Steephen. 2011. Excitability range of medium spiny neurons widens through the combined effects of inward rectifying potassium current inactivation and dopaminergic modulation. *Neurocomputing* . [CrossRef]
43. Alexandre L. Madureira, Daniele Q.M. Madureira, Pedro O. Pinheiro. 2011. A multiscale numerical method for the heterogeneous cable equation. *Neurocomputing* . [CrossRef]
44. Kendall H Lee, Frederick L Hitti, Su-Youne Chang, Dongchul C Lee, David W Roberts, Cameron C McIntyre, James C Leiter. 2011. High frequency stimulation abolishes thalamic network oscillations: an electrophysiological and computational analysis. *Journal of Neural Engineering* **8**:4, 046001. [CrossRef]
45. Patrick Crotty, Thomas Sangrey. 2011. Optimization of battery strengths in the Hodgkin–Huxley model. *Neurocomputing* . [CrossRef]
46. E J Peterson, O Izad, D J Tyler. 2011. Predicting myelinated axon activation using spatial characteristics of the extracellular field. *Journal of Neural Engineering* **8**:4, 046030. [CrossRef]
47. Alexander D. Rast, Javier Navaridas, Xin Jin, Francesco Galluppi, Luis A. Plana, Jose Miguel-Alonso, Cameron Patterson, Mikel Luján, Steve Furber. 2011. Managing Burstiness and Scalability in Event-Driven Models on the SpiNNaker Neuromimetic System. *International Journal of Parallel Programming* . [CrossRef]
48. Johannes Luthman, Freek E. Hoebeek, Reinoud Maex, Neil Davey, Rod Adams, Chris I. Zeeuw, Volker Steuber. 2011. STD-Dependent and Independent Encoding of Input Irregularity as Spike Rate in a Computational Model of a Cerebellar Nucleus Neuron. *The Cerebellum* . [CrossRef]
49. Takayuki Kannon, Keiichiro Inagaki, Nilton L. Kamiji, Kouji Makimura, Shiro Usui. 2011. PLATO: Data-oriented approach to collaborative large-scale brain system modeling. *Neural Networks* . [CrossRef]
50. Amorn Wongsarnpigoon, Warren M. Grill. 2011. Computer-based model of epidural motor cortex stimulation: Effects of electrode position and geometry on activation of cortical neurons. *Clinical Neurophysiology* . [CrossRef]
51. Martha W. Bagnall, Court Hull, Eric A. Bushong, Mark H. Ellisman, Massimo Scanziani. 2011. Multiple Clusters of Release Sites Formed by Individual Thalamic Afferents onto Cortical Interneurons Ensure Reliable Transmission. *Neuron* **71**:1, 180-194. [CrossRef]
52. Joshua L Plotkin, Michelle Day, D James Surmeier. 2011. Synaptically driven state transitions in distal dendrites of striatal spiny neurons. *Nature Neuroscience* . [CrossRef]
53. Benjamin D. Ausdenmoore, Zachary A. Markwell, David R. Ladle. 2011. Localization of presynaptic inputs on dendrites of individually labeled neurons in three dimensional space using a center distance algorithm. *Journal of Neuroscience Methods* . [CrossRef]
54. Christopher R Butson, Ian O Miller, Richard A Normann, Gregory A Clark. 2011. Selective neural activation in a histologically derived model of peripheral nerve. *Journal of Neural Engineering* **8**:3, 036009. [CrossRef]
55. D.B. Jaffe, B. Wang, R. Brenner. 2011. Shaping of action potentials by type I and type II large-conductance Ca2+-activated K+ channels. *Neuroscience* . [CrossRef]
56. Stefan Lang, Vincent J. Dercksen, Bert Sakmann, Marcel Oberlaender. 2011. Simulation of signal flow in 3D reconstructions of an anatomically realistic neural network in rat vibrissal cortex. *Neural Networks* . [CrossRef]
57. A.V. Masurkar, W.R. Chen. 2011. Potassium currents of olfactory bulb juxtaglomerular cells: characterization, simulation, and implications for plateau potential firing. *Neuroscience* . [CrossRef]
58. Qingfei Luo, Xia Jiang, Bin Chen, Yi Zhu, Jia-Hong Gao. 2011. Modeling neuronal current MRI signal with human neuron. *Magnetic Resonance in Medicine* **65**:6, 1680-1689. [CrossRef]
59. Sergiy Kochubey, Alexey Semyanov, Leonid Savtchenko. 2011. Network with shunting synapses as a non-linear frequency modulator. *Neural Networks* **24**:5, 407-416. [CrossRef]
60. A.V. Masurkar, W.R. Chen. 2011. Calcium currents of olfactory bulb juxtaglomerular cells: Profile and multiple conductance plateau potential simulation. *Neuroscience* . [CrossRef]
61. Konstantinos Xylouris, Gillian Queisser, Gabriel Wittum. 2011. A three-dimensional mathematical model of active signal processing in axons. *Computing and Visualization in Science* . [CrossRef]
62. Maximiliano Josè Nigro, Paola Perin, Jacopo Magistretti. 2011. Differential effects of Zn2+ on activation, deactivation, and inactivation kinetics in neuronal voltage-gated Na+ channels. *Pflügers Archiv - European Journal of Physiology* . [CrossRef]
63. Natalia Toporikova, Tzu-Hsin Tsao, Terrence Michael Wright, Robert J. Butera. 2011. Conflicting effects of excitatory synaptic and electric coupling on the dynamics of square-wave bursters. *Journal of Computational Neuroscience* . [CrossRef]
64. Dongchul Lee, Brad Hershey, Kerry Bradley, Thomas Yearwood. 2011. Predicted effects of pulse width programming in spinal cord stimulation: a mathematical modeling study. *Medical & Biological Engineering & Computing* . [CrossRef]

65. Hiroki Akiyama, Yuki Shimizu, Hiroyoshi Miyakawa, Masashi Inoue. 2011. Extracellular DC electric fields induce nonuniform membrane polarization in rat hippocampal CA1 pyramidal neurons. *Brain Research* **1383**, 22-35. [CrossRef]
66. J.A. Bailey, R. Wilcock, P.R. Wilson, J.E. Chad. 2011. Behavioral simulation and synthesis of biological neuron systems using synthesizable VHDL. *Neurocomputing* . [CrossRef]
67. Wei Yao, Huaxiong Huang, Robert M. Miura. 2011. A Continuum Neuronal Model for the Instigation and Propagation of Cortical Spreading Depression. *Bulletin of Mathematical Biology* . [CrossRef]
68. Elena È. Saftenku. 2011. Effects of Calretinin on Ca2+ Signals in Cerebellar Granule Cells: Implications of Cooperative Ca2+ Binding. *The Cerebellum* . [CrossRef]
69. Tiago Branco, Michael Häusser. 2011. Synaptic Integration Gradients in Single Cortical Pyramidal Cell Dendrites. *Neuron* **69**:5, 885-892. [CrossRef]
70. Sherry-Ann Brown, Ion I. Moraru, James C. Schaff, Leslie M. Loew. 2011. Virtual NEURON: a strategy for merged biochemical and electrophysiological modeling. *Journal of Computational Neuroscience* . [CrossRef]
71. S. A. Kochubey, L. P. Savtchenko, A. V. Sem'yanov. 2011. Modulation of Oscillatory Synchronization in an Interneuronal Network under the Influence of Tonic GABA-ergic Inhibition: a Model Study. *Neurophysiology* . [CrossRef]
72. Ivan Pavlov, Annalisa Scimemi, Leonid Savtchenko, Dimitri M. Kullmann, Matthew C. Walker. 2011. Ih-mediated depolarization enhances the temporal precision of neuronal integration. *Nature Communications* **2**, 199. [CrossRef]
73. Marc de Kamps. 2011. Towards truly human-level intelligence in artificial applications. *Cognitive Systems Research* . [CrossRef]
74. Tobias Huth, Andrea Rittger, Paul Saftig, Christian Alzheimer. 2011. #-Site APP-cleaving enzyme 1 (BACE1) cleaves cerebellar Na+ channel #4-subunit and promotes Purkinje cell firing by slowing the decay of resurgent Na+ current. *Pflügers Archiv - European Journal of Physiology* . [CrossRef]
75. Jay S Coggan, Gabriel K Ocker, Steven A Prescott, Terrence J Sejnowski. 2011. Complex symptoms of demyelination and nerve damage explained by nonlinear dynamical analysis of conductance-based models. *BMC Neuroscience* **12**:Suppl 1, P292. [CrossRef]
76. J. Luis Lujan, Ashutosh Chaturvedi, Donald A. Malone, Ali R. Rezai, Andre G. Machado, Cameron C. McIntyre. 2011. Axonal pathways linked to therapeutic and nontherapeutic outcomes during psychiatric deep brain stimulation. *Human Brain Mapping* n/a-n/a. [CrossRef]
77. Philipp Rautenberg, Andrey Sobolev, Andreas VM Herz, Thomas Wachtler. 2011. Automated generation of compartmental models via database tools for neurophysiology data management, analysis, and simulation. *BMC Neuroscience* **12**:Suppl 1, P366. [CrossRef]
78. Mark EJ Sheffield, Tyler K Best, Brett D Mensh, William L Kath, Nelson Spruston. 2011. Slow integration leads to persistent action potential firing in distal axons of coupled interneurons. *BMC Neuroscience* **12**:Suppl 1, O17. [CrossRef]
79. Rongjing Ge, Hao Qian, Jin-hui Wang. 2011. Physiological synaptic signals initiate sequential spikes at soma of cortical pyramidal neurons. *Molecular Brain* **4**:1, 19. [CrossRef]
80. Mark E J Sheffield, Tyler K Best, Brett D Mensh, William L Kath, Nelson Spruston. 2010. Slow integration leads to persistent action potential firing in distal axons of coupled interneurons. *Nature Neuroscience* . [CrossRef]
81. Michiel W. H. Remme, John Rinzel. 2010. Role of active dendritic conductances in subthreshold input integration. *Journal of Computational Neuroscience* . [CrossRef]
82. Peter Jedlicka, Thomas Deller, Stephan W. Schwarzacher. 2010. Computational modeling of GABAA receptor-mediated paired-pulse inhibition in the dentate gyrus. *Journal of Computational Neuroscience* **29**:3, 509-519. [CrossRef]
83. Claude Bédard, Serafim Rodrigues, Noah Roy, Diego Contreras, Alain Destexhe. 2010. Evidence for frequency-dependent extracellular impedance from the transfer function between extracellular and intracellular potentials. *Journal of Computational Neuroscience* **29**:3, 389-403. [CrossRef]
84. Tianhe C Zhang, Warren M Grill. 2010. Modeling deep brain stimulation: point source approximation versus realistic representation of the electrode. *Journal of Neural Engineering* **7**:6, 066009. [CrossRef]
85. Kiran Nataraj, Nicolas Le Roux, Marc Nahmani, Sandrine Lefort, Gina Turrigiano. 2010. Visual Deprivation Suppresses L5 Pyramidal Neuron Excitability by Preventing the Induction of Intrinsic Plasticity. *Neuron* **68**:4, 750-762. [CrossRef]
86. Peadar F. Grant, Madeleine M. Lowery. 2010. Effect of Dispersive Conductivity and Permittivity in Volume Conductor Models of Deep Brain Stimulation. *IEEE Transactions on Biomedical Engineering* **57**:10, 2386-2393. [CrossRef]

87. Reza Zomorrodi, Alex S. Ferecskó, Krisztina Kovács, Helmut Kröger, Igor Timofeev. 2010. Analysis of morphological features of thalamocortical neurons from the ventroposterolateral nucleus of the cat. *The Journal of Comparative Neurology* **518**:17, 3541-3556. [CrossRef]
88. Chandra Prakash Poudyal, Chandong Chang, Hyun-Joo Oh, Saro Lee. 2010. Landslide susceptibility maps comparing frequency ratio and artificial neural networks: a case study from the Nepal Himalaya. *Environmental Earth Sciences* **61**:5, 1049-1064. [CrossRef]
89. S. Renaud, J. Tomas, N. Lewis, Y. Bornat, A. Daouzli, M. Rudolph, A. Destexhe, S. Saïghi. 2010. PAX: A mixed hardware/ software simulation platform for spiking neural networks. *Neural Networks* **23**:7, 905-916. [CrossRef]
90. Jeffrey Seely, Patrick Crotty. 2010. Optimization of the leak conductance in the squid giant axon. *Physical Review E* **82**:2. . [CrossRef]
91. Amorn Wongsarnpigoon, Warren M Grill. 2010. Energy-efficient waveform shapes for neural stimulation revealed with a genetic algorithm. *Journal of Neural Engineering* **7**:4, 046009. [CrossRef]
92. R.J. Sadleir, S.C. Grant, E.J. Woo. 2010. Can high-field MREIT be used to directly detect neural activity? Theoretical considerations. *NeuroImage* **52**:1, 205-216. [CrossRef]
93. C. Shilyansky, K. H. Karlsgodt, D. M. Cummings, K. Sidiropoulou, M. Hardt, A. S. James, D. Ehninger, C. E. Bearden, P. Poirazi, J. D. Jentsch, T. D. Cannon, M. S. Levine, A. J. Silva. 2010. Neurofibromin regulates corticostriatal inhibitory networks during working memory performance. *Proceedings of the National Academy of Sciences* **107**:29, 13141-13146. [CrossRef]
94. Ilya A Fleidervish, Nechama Lasser-Ross, Michael J Gutnick, William N Ross. 2010. Na+ imaging reveals little difference in action potential–evoked Na+ influx between axon and soma. *Nature Neuroscience* **13**:7, 852-860. [CrossRef]
95. Michael London, Arnd Roth, Lisa Beeren, Michael Häusser, Peter E. Latham. 2010. Sensitivity to perturbations in vivo implies high noise and suggests rate coding in cortex. *Nature* **466**:7302, 123-127. [CrossRef]
96. Matthew S. Grubb, Juan Burrone. 2010. Activity-dependent relocation of the axon initial segment fine-tunes neuronal excitability. *Nature* **465**:7301, 1070-1074. [CrossRef]
97. R. Angus Silver. 2010. Neuronal arithmetic. *Nature Reviews Neuroscience* **11**:7, 474-489. [CrossRef]
98. P. Jedlicka, M. Hoon, T. Papadopoulos, A. Vlachos, R. Winkels, A. Poulopoulos, H. Betz, T. Deller, N. Brose, F. Varoqueaux, S. W. Schwarzacher. 2010. Increased Dentate Gyrus Excitability in Neuroligin-2-Deficient Mice in Vivo. *Cerebral Cortex* . [CrossRef]
99. Amorn Wongsarnpigoon, John P Woock, Warren M Grill. 2010. Efficiency Analysis of Waveform Shape for Electrical Excitation of Nerve Fibers. *IEEE Transactions on Neural Systems and Rehabilitation Engineering* **18**:3, 319-328. [CrossRef]
100. Ulysses Bernardet, Paul F. M. J. Verschure. 2010. iqr: A Tool for the Construction of Multi-level Simulations of Brain and Behaviour. *Neuroinformatics* **8**:2, 113-134. [CrossRef]
101. Anna Y. Kuznetsova, Marco A. Huertas, Alexey S. Kuznetsov, Carlos A. Paladini, Carmen C. Canavier. 2010. Regulation of firing frequency in a computational model of a midbrain dopaminergic neuron. *Journal of Computational Neuroscience* **28**:3, 389-403. [CrossRef]
102. Michiel W.H. Remme, Máté Lengyel, Boris S. Gutkin. 2010. Democracy-Independence Trade-Off in Oscillating Dendrites and Its Implications for Grid Cells. *Neuron* **66**:3, 429-437. [CrossRef]
103. Jen-Yung Chen. 2010. A Simulation Study Investigating the Impact of Dendritic Morphology and Synaptic Topology on Neuronal Firing Patterns. *Neural Computation* **22**:4, 1086-1111. [Abstract] [Full Text] [PDF] [PDF Plus]
104. Ashutosh Chaturvedi, Christopher R. Butson, Scott F. Lempka, Scott E. Cooper, Cameron C. McIntyre. 2010. Patient-specific models of deep brain stimulation: Influence of field model complexity on neural activation predictions. *Brain Stimulation* **3**:2, 65-77. [CrossRef]
105. David Cofer, Gennady Cymbalyuk, James Reid, Ying Zhu, William J. Heitler, Donald H. Edwards. 2010. AnimatLab: A 3D graphics environment for neuromechanical simulations. *Journal of Neuroscience Methods* **187**:2, 280-288. [CrossRef]
106. William N. Grimes, Jun Zhang, Cole W. Graydon, Bechara Kachar, Jeffrey S. Diamond. 2010. Retinal Parallel Processors: More than 100 Independent Microcircuits Operate within a Single Interneuron. *Neuron* **65**:6, 873-885. [CrossRef]
107. Chao Liu, Qian Li, Yuanyuan Su, Lan Bao. 2010. Prostaglandin E 2 Promotes Na v 1.8 Trafficking via Its Intracellular RRR Motif Through the Protein Kinase A Pathway. *Traffic* **11**:3, 405-417. [CrossRef]
108. Brian W. Jarecki, Andrew D. Piekarz, James O. Jackson, Theodore R. Cummins. 2010. Human voltage-gated sodium channel mutations that cause inherited neuronal and muscle channelopathies increase resurgent sodium currents. *Journal of Clinical Investigation* **120**:1, 369-378. [CrossRef]

109. Patrick J. C. May, Hannu Tiitinen. 2010. Mismatch negativity (MMN), the deviance-elicited auditory deflection, explained. *Psychophysiology* **47**:1, 66-122. [CrossRef]
110. J. S. Coggan, S. A. Prescott, T. M. Bartol, T. J. Sejnowski. 2010. Inaugural Article: Imbalance of ionic conductances contributes to diverse symptoms of demyelination. *Proceedings of the National Academy of Sciences* **107**:48, 20602. [CrossRef]
111. Leslie M. Loew, James C. Schaff, Boris M. Slepchenko, Ion I. MoraruThe Virtual Cell Project 273-288. [CrossRef]
112. S. Chemla, F. Chavane. 2010. Voltage-sensitive dye imaging: Technique review and models. *Journal of Physiology-Paris* **104**:1-2, 40-50. [CrossRef]
113. Amane Koizumi, Tatjana C. Jakobs, Richard H. Masland. 2010. A mosaic of synaptic contacts among three retinal neurons. *The Journal of Comparative Neurology* n/a-n/a. [CrossRef]
114. Andreas Bahmer, Gerald Langner. 2010. Parameters for a model of an oscillating neuronal network in the cochlear nucleus defined by genetic algorithms. *Biological Cybernetics* **102**:1, 81-93. [CrossRef]
115. M. G. Sheroziya, A. V. Egorov. 2010. Effects of Extracellular Calcium on the Volley Activity of Entorhinal Cortex Neurons in Neonatal Rats: Computer Simulation. *Neuroscience and Behavioral Physiology* **40**:1, 1-4. [CrossRef]
116. A. Hai, A. Dormann, J. Shappir, S. Yitzchaik, C. Bartic, G. Borghs, J. P. M. Langedijk, M. E. Spira. 2009. Spine-shaped gold protrusions improve the adherence and electrical coupling of neurons with the surface of micro-electronic devices. *Journal of The Royal Society Interface* **6**:41, 1153-1165. [CrossRef]
117. Alain Destexhe. 2009. Self-sustained asynchronous irregular states and Up–Down states in thalamic, cortical and thalamocortical networks of nonlinear integrate-and-fire neurons. *Journal of Computational Neuroscience* **27**:3, 493-506. [CrossRef]
118. John Eric Steephen, Rohit Manchanda. 2009. Differences in biophysical properties of nucleus accumbens medium spiny neurons emerging from inactivation of inward rectifying potassium currents. *Journal of Computational Neuroscience* **27**:3, 453-470. [CrossRef]
119. Juan Martinez, Carlos Pedreira, Matias J. Ison, Rodrigo Quian Quiroga. 2009. Realistic simulation of extracellular recordings. *Journal of Neuroscience Methods* **184**:2, 285-293. [CrossRef]
120. Thomas Kuenzel, Marcus J. Wirth, Harald Luksch, Hermann Wagner, Jörg Mey. 2009. Increase of Kv3.1b expression in avian auditory brainstem neurons correlates with synaptogenesis in vivo and in vitro. *Brain Research* **1302**, 64-75. [CrossRef]
121. Hayriye Cagnan, Hil G. E. Meijer, Stephan A. Van Gils, Martin Krupa, Tjitske Heida, Michelle Rudolph, Wytse J. Wadman, Hubert C. F. Martens. 2009. Frequency-selectivity of a thalamocortical relay neuron during Parkinson's disease and deep brain stimulation: a computational study. *European Journal of Neuroscience* **30**:7, 1306-1317. [CrossRef]
122. D. Michael Ackermann, Emily L. Foldes, Niloy Bhadra, Kevin L. Kilgore. 2009. Effect of Bipolar Cuff Electrode Design on Block Thresholds in High-Frequency Electrical Neural Conduction Block. *IEEE Transactions on Neural Systems and Rehabilitation Engineering* **17**:5, 469-477. [CrossRef]
123. V. Menon, N. Spruston, W. L. Kath. 2009. A state-mutating genetic algorithm to design ion-channel models. *Proceedings of the National Academy of Sciences* **106**:39, 16829-16834. [CrossRef]
124. Simon P. Peron, Peter W. Jones, Fabrizio Gabbiani. 2009. Precise Subcellular Input Retinotopy and Its Computational Consequences in an Identified Visual Interneuron. *Neuron* **63**:6, 830-842. [CrossRef]
125. Randal A. Koene, Betty Tijms, Peter Hees, Frank Postma, Alexander Ridder, Ger J. A. Ramakers, Jaap Pelt, Arjen Ooyen. 2009. NETMORPH: A Framework for the Stochastic Generation of Large Scale Neuronal Networks With Realistic Neuron Morphologies. *Neuroinformatics* **7**:3, 195-210. [CrossRef]
126. Wenqin Hu, Cuiping Tian, Tun Li, Mingpo Yang, Han Hou, Yousheng Shu. 2009. Distinct contributions of Nav1.6 and Nav1.2 in action potential initiation and backpropagation. *Nature Neuroscience* **12**:8, 996-1002. [CrossRef]
127. Yael Katz, Vilas Menon, Daniel A. Nicholson, Yuri Geinisman, William L. Kath, Nelson Spruston. 2009. Synapse Distribution Suggests a Two-Stage Model of Dendritic Integration in CA1 Pyramidal Neurons. *Neuron* **63**:2, 171-177. [CrossRef]
128. Raphael Winkels, Peter Jedlicka, Felix K. Weise, Christian Schultz, Thomas Deller, Stephan W. Schwarzacher. 2009. Reduced excitability in the dentate gyrus network of #IV-spectrin mutant mice in vivo. *Hippocampus* **19**:7, 677-686. [CrossRef]
129. Edén Flores-Barrera, Antonio Laville, Victor Plata, Dagoberto Tapia, José Bargas, Elvira Galarraga. 2009. Inhibitory Contribution to Suprathreshold Corticostriatal Responses: An Experimental and Modeling Study. *Cellular and Molecular Neurobiology* **29**:5, 719-731. [CrossRef]

130. Yoko Tominaga, Michinori Ichikawa, Takashi Tominaga. 2009. Membrane potential response profiles of CA1 pyramidal cells probed with voltage-sensitive dye optical imaging in rat hippocampal slices reveal the impact of GABAA-mediated feed-forward inhibition in signal propagation. *Neuroscience Research* **64**:2, 152-161. [CrossRef]
131. Hirokazu Takahashi, Masayuki Nakao, Kimitaka Kaga. 2009. Simulation of nerve bundle activation by simultaneous multipoint extracellular stimulation with surface electrodes. *Electronics and Communications in Japan* **92**:6, 31-40. [CrossRef]
132. Amin Mahnam, S Mohammad Reza Hashemi, Warren M Grill. 2009. Measurement of the current–distance relationship using a novel refractory interaction technique. *Journal of Neural Engineering* **6**:3, 036005. [CrossRef]
133. Walther Akemann, Alicia Lundby, Hiroki Mutoh, Thomas Knöpfel. 2009. Effect of Voltage Sensitive Fluorescent Proteins on Neuronal Excitability. *Biophysical Journal* **96**:10, 3959-3976. [CrossRef]
134. Sébastien Joucla, Blaise Yvert. 2009. The "Mirror" Estimate: An Intuitive Predictor of Membrane Polarization during Extracellular Stimulation. *Biophysical Journal* **96**:9, 3495-3508. [CrossRef]
135. Toshiaki Omori, Toru Aonishi, Hiroyoshi Miyakawa, Masashi Inoue, Masato Okada. 2009. Steep decrease in the specific membrane resistance in the apical dendrites of hippocampal CA1 pyramidal neurons. *Neuroscience Research* **64**:1, 83-95. [CrossRef]
136. P. Hemond, M. Migliore, G.A. Ascoli, D.B. Jaffe. 2009. The membrane response of hippocampal CA3b pyramidal neurons near rest: Heterogeneity of passive properties and the contribution of hyperpolarization-activated currents. *Neuroscience* **160**:2, 359-370. [CrossRef]
137. Klaus M. Stiefel, Boris S. Gutkin, Terrence J. Sejnowski. 2009. The effects of cholinergic neuromodulation on neuronal phase-response curves of modeled cortical neurons. *Journal of Computational Neuroscience* **26**:2, 289-301. [CrossRef]
138. E.È. Saftenku. 2009. Computational study of non-homogeneous distribution of Ca2+ handling systems in cerebellar granule cells. *Journal of Theoretical Biology* **257**:2, 228-244. [CrossRef]
139. U. Frey, U. Egert, F. Heer, S. Hafizovic, A. Hierlemann. 2009. Microelectronic system for high-resolution mapping of extracellular electric fields applied to brain slices. *Biosensors and Bioelectronics* **24**:7, 2191-2198. [CrossRef]
140. Tiago P. Carvalho, Dean V. Buonomano. 2009. Differential Effects of Excitatory and Inhibitory Plasticity on Synaptically Driven Neuronal Input-Output Functions. *Neuron* **61**:5, 774-785. [CrossRef]
141. P. Wulff, A. A. Ponomarenko, M. Bartos, T. M. Korotkova, E. C. Fuchs, F. Bahner, M. Both, A. B. L. Tort, N. J. Kopell, W. Wisden, H. Monyer. 2009. Hippocampal theta rhythm and its coupling with gamma oscillations require fast inhibition onto parvalbumin-positive interneurons. *Proceedings of the National Academy of Sciences* **106**:9, 3561-3566. [CrossRef]
142. H. Steven Colburn, Yoojin Chung, Yi Zhou, Andrew Brughera. 2009. Models of Brainstem Responses to Bilateral Electrical Stimulation. *Journal of the Association for Research in Otolaryngology* **10**:1, 91-110. [CrossRef]
143. Béatrice Marcelin, Laëtitia Chauvière, Albert Becker, Michele Migliore, Monique Esclapez, Christophe Bernard. 2009. h channel-dependent deficit of theta oscillation resonance and phase shift in temporal lobe epilepsy. *Neurobiology of Disease* **33**:3, 436-447. [CrossRef]
144. Tariq Zahid, Frances K. Skinner. 2009. Predicting synchronous and asynchronous network groupings of hippocampal interneurons coupled with dendritic gap junctions. *Brain Research* **1262**, 115-129. [CrossRef]
145. Jason S. Rothman, Laurence Cathala, Volker Steuber, R. Angus Silver. 2009. Synaptic depression enables neuronal gain control. *Nature* **457**:7232, 1015-1018. [CrossRef]
146. G. G. Somjen, H. Kager, W. J. Wadman. 2009. Calcium sensitive non-selective cation current promotes seizure-like discharges and spreading depression in a model neuron. *Journal of Computational Neuroscience* **26**:1, 139-147. [CrossRef]
147. M. Pospischil, Z. Piwkowska, T. Bal, A. Destexhe. 2009. Extracting synaptic conductances from single membrane potential traces. *Neuroscience* **158**:2, 545-552. [CrossRef]
148. Martin Pospischil, Zuzanna Piwkowska, Thierry Bal, Alain Destexhe. 2009. Characterizing neuronal activity by describing the membrane potential as a stochastic process. *Journal of Physiology-Paris* **103**:1-2, 98-106. [CrossRef]
149. Vassilis Cutsuridis, Stuart Cobb, Bruce P. Graham. 2009. Encoding and retrieval in a model of the hippocampal CA1 microcircuit. *Hippocampus* NA-NA. [CrossRef]
150. Masaaki Takahashi, Kiyohisa Natsume. 2009. Automatic Estimation of the Dynamics of Channel Conductance Using a Recurrent Neural Network. *Advances in Artificial Neural Systems* **2009**, 1-11. [CrossRef]
151. Kalyan V. Srinivas, Sujit K. Sikdar. 2008. Epileptiform activity induces distance-dependent alterations of the Ca 2+ extrusion mechanism in the apical dendrites of subicular pyramidal neurons. *European Journal of Neuroscience* **28**:11, 2195-2212. [CrossRef]

152. Michael L. Hines, Henry Markram, Felix Schürmann. 2008. Fully implicit parallel simulation of single neurons. *Journal of Computational Neuroscience* **25**:3, 439-448. [CrossRef]
153. Michael J. Rempe, Nelson Spruston, William L. Kath, David L. Chopp. 2008. Compartmental neural simulations with spatial adaptivity. *Journal of Computational Neuroscience* **25**:3, 465-480. [CrossRef]
154. V. Gonzalez-Perez, A. Neely, C. Tapia, G. Gonzalez-Gutierrez, G. Contreras, P. Orio, V. Lagos, G. Rojas, T. Estevez, K. Stack, D. Naranjo. 2008. Slow Inactivation in Shaker K Channels Is Delayed by Intracellular Tetraethylammonium. *The Journal of General Physiology* **132**:6, 633-650. [CrossRef]
155. J. Devaux, A. Gow. 2008. Tight junctions potentiate the insulative properties of small CNS myelinated axons. *The Journal of Cell Biology* **183**:5, 909-921. [CrossRef]
156. I. A. Fleidervish, L. Libman, E. Katz, M. J. Gutnick. 2008. Endogenous polyamines regulate cortical neuronal excitability by blocking voltage-gated Na+ channels. *Proceedings of the National Academy of Sciences* **105**:48, 18994-18999. [CrossRef]
157. Michele Migliore, Gaspare Novara, Domenico Tegolo. 2008. Single neuron binding properties and the magical number 7. *Hippocampus* **18**:11, 1122-1130. [CrossRef]
158. W. Geit, E. Schutter, P. Achard. 2008. Automated neuron model optimization techniques: a review. *Biological Cybernetics* **99**:4-5, 241-251. [CrossRef]
159. Alexander Gow, Jerome Devaux. 2008. A model of tight junction function in central nervous system myelinated axons. *Neuron Glia Biology* **4**:04, 307. [CrossRef]
160. Martin Pospischil, Maria Toledo-Rodriguez, Cyril Monier, Zuzanna Piwkowska, Thierry Bal, Yves Frégnac, Henry Markram, Alain Destexhe. 2008. Minimal Hodgkin–Huxley type models for different classes of cortical and thalamic neurons. *Biological Cybernetics* **99**:4-5, 427-441. [CrossRef]
161. Paolo Massobrio, Sergio Martinoia. 2008. Modelling small-patterned neuronal networks coupled to microelectrode arrays. *Journal of Neural Engineering* **5**:3, 350-359. [CrossRef]
162. Courtney L. Lopreore, Thomas M. Bartol, Jay S. Coggan, Daniel X. Keller, Gina E. Sosinsky, Mark H. Ellisman, Terrence J. Sejnowski. 2008. Computational Modeling of Three-Dimensional Electrodiffusion in Biological Systems: Application to the Node of Ranvier. *Biophysical Journal* **95**:6, 2624-2635. [CrossRef]
163. S C Bellinger, G Miyazawa, P N Steinmetz. 2008. Submyelin potassium accumulation may functionally block subsets of local axons during deep brain stimulation: a modeling study. *Journal of Neural Engineering* **5**:3, 263-274. [CrossRef]
164. Hui Lu, Cynthia A Chestek, Kendrick M Shaw, Hillel J Chiel. 2008. Selective extracellular stimulation of individual neurons in ganglia. *Journal of Neural Engineering* **5**:3, 287-309. [CrossRef]
165. A MAHNAM, S HASHEMI, W GRILL. 2008. Computational evaluation of methods for measuring the spatial extent of neural activation. *Journal of Neuroscience Methods* **173**:1, 153-164. [CrossRef]
166. M. Helmstaedter, B. Sakmann, D. Feldmeyer. 2008. The Relation between Dendritic Geometry, Electrical Excitability, and Axonal Projections of L2/3 Interneurons in Rat Barrel Cortex. *Cerebral Cortex* **19**:4, 938-950. [CrossRef]
167. T. Bessaih, N. Leresche, R. C. Lambert. 2008. T current potentiation increases the occurrence and temporal fidelity of synaptically evoked burst firing in sensory thalamic neurons. *Proceedings of the National Academy of Sciences* **105**:32, 11376-11381. [CrossRef]
168. Joshua N. Milstein, Christof Koch. 2008. Dynamic Moment Analysis of the Extracellular Electric Field of a Biologically Realistic Spiking Neuron. *Neural Computation* **20**:8, 2070-2084. [Abstract] [PDF] [PDF Plus]
169. Magteld Zeitler, Pascal Fries, Stan Gielen. 2008. Biased competition through variations in amplitude of #-oscillations. *Journal of Computational Neuroscience* **25**:1, 89-107. [CrossRef]
170. Michael L. Hines, Hubert Eichner, Felix Schürmann. 2008. Neuron splitting in compute-bound parallel network simulations enables runtime scaling with twice as many processors. *Journal of Computational Neuroscience* **25**:1, 203-210. [CrossRef]
171. A.M. Cassarà, B. Maraviglia. 2008. Microscopic investigation of the resonant mechanism for the implementation of nc-MRI at ultra-low field MRI. *NeuroImage* **41**:4, 1228-1241. [CrossRef]
172. F. Saraga, T. Balena, T. Wolansky, C.T. Dickson, M.A. Woodin. 2008. Inhibitory synaptic plasticity regulates pyramidal neuron spiking in the rodent hippocampus. *Neuroscience* **155**:1, 64-75. [CrossRef]
173. Steven D. Buckingham, Andrew N. Spencer. 2008. Action potential shape change in an electrically coupled network during propagation: a computer simulation. *Invertebrate Neuroscience* **8**:2, 83-89. [CrossRef]
174. S. Kochubey, L. Savtchenko. 2008. Geometrical size of the neuronal network plays a key role in synchronization of its activity. *Neurophysiology* **40**:3, 224-227. [CrossRef]

175. Daniel K. Hartline. 2008. What is myelin?. *Neuron Glia Biology* **4**:02, 153. [CrossRef]
176. S HUGHES, M LORINCZ, D COPE, V CRUNELLI. 2008. NeuReal: An interactive simulation system for implementing artificial dendrites and large hybrid networks. *Journal of Neuroscience Methods* **169**:2, 290-301. [CrossRef]
177. Z PIWKOWSKA, M POSPISCHIL, R BRETTE, J SLIWA, M RUDOLPHLILITH, T BAL, A DESTEXHE. 2008. Characterizing synaptic conductance fluctuations in cortical neurons and their influence on spike generation. *Journal of Neuroscience Methods* **169**:2, 302-322. [CrossRef]
178. R. J. Morgan, I. Soltesz. 2008. From the Cover: Nonrandom connectivity of the epileptic dentate gyrus predicts a major role for neuronal hubs in seizures. *Proceedings of the National Academy of Sciences* **105**:16, 6179-6184. [CrossRef]
179. M. Migliore, Gordon M. Shepherd. 2008. Dendritic action potentials connect distributed dendrodendritic microcircuits. *Journal of Computational Neuroscience* **24**:2, 207-221. [CrossRef]
180. Peter Hemond, Daniel Epstein, Angela Boley, Michele Migliore, Giorgio A. Ascoli, David B. Jaffe. 2008. Distinct classes of pyramidal cells exhibit mutually exclusive firing patterns in hippocampal area CA3b. *Hippocampus* **18**:4, 411-424. [CrossRef]
181. Ricardo Escola, Christophe Pouzat, Antoine Chaffiol, Blaise Yvert, Isabelle E. Magnin, R#gis Guillemaud. 2008. SIMONE: A Realistic Neural Network Simulator to Reproduce MEA-Based Recordings. *IEEE Transactions on Neural Systems and Rehabilitation Engineering* **16**:2, 149-160. [CrossRef]
182. Chad A Bossetti, Merrill J Birdno, Warren M Grill. 2008. Analysis of the quasi-static approximation for calculating potentials generated by neural stimulation. *Journal of Neural Engineering* **5**:1, 44-53. [CrossRef]
183. Ilya A Fleidervish, Lior Libman. 2008. How cesium dialysis affects the passive properties of pyramidal neurons: implications for voltage clamp studies of persistent sodium current. *New Journal of Physics* **10**:3, 035001. [CrossRef]
184. Yifat Kovalsky, Ron Amir, Marshall Devor. 2008. Subthreshold oscillations facilitate neuropathic spike discharge by overcoming membrane accommodation. *Experimental Neurology* **210**:1, 194-206. [CrossRef]
185. David J. Sandstrom. 2008. Isoflurane Reduces Excitability of Drosophila Larval Motoneurons by Activating a Hyperpolarizing Leak Conductance. *Anesthesiology* **108**:3, 434-446. [CrossRef]
186. Claude Bédard, Alain Destexhe. 2008. A Modified Cable Formalism for Modeling Neuronal Membranes at High Frequencies. *Biophysical Journal* **94**:4, 1133-1143. [CrossRef]
187. Eugenia Chen, Klaus M. Stiefel, Terrence J. Sejnowski, Theodore H. Bullock. 2008. Model of traveling waves in a coral nerve network. *Journal of Comparative Physiology A* **194**:2, 195-200. [CrossRef]
188. Jay Spampanato, Alan L. GoldinComputer Simulations of Sodium Channel Mutations that Cause Generalized Epilepsy with Febrile Seizures Plus 143-154. [CrossRef]
189. Gianmaria MaccaferriComplex Synaptic Dynamics of GABAergic Networks of the Hippocampus 288-303. [CrossRef]
190. Dezhe Z Jin. 2008. Decoding spatiotemporal spike sequences via the finite state automata dynamics of spiking neural networks. *New Journal of Physics* **10**:1, 015010. [CrossRef]
191. F Weber, H Eichner, H Cuntz, A Borst. 2008. Eigenanalysis of a neural network for optic flow processing. *New Journal of Physics* **10**:1, 015013. [CrossRef]
192. Maxim Bazhenov, Arthur R. Houweling, Igor Timofeev, Terrence J. SejnowskiHomeostatic Plasticity and post-Traumatic Epileptogenesis 259-IX. [CrossRef]
193. Padraig Gleeson, Volker Steuber, R. Angus SilverUsing Neuroconstruct to Develop and Modify Biologically Detailed 3D Neuronal Network Models in Health and Disease 48-V. [CrossRef]
194. Christopher R. Butson, Cameron C. McIntyre. 2008. Current steering to control the volume of tissue activated during deep brain stimulation. *Brain Stimulation* **1**:1, 7-15. [CrossRef]
195. A.M. Cassarà, G.E. Hagberg, M. Bianciardi, M. Migliore, B. Maraviglia. 2008. Realistic simulations of neuronal activity: A contribution to the debate on direct detection of neuronal currents by MRI. *NeuroImage* **39**:1, 87-106. [CrossRef]
196. N.T. Carnevale, Michael HinesThe Neuron Simulation Environment in Epilepsy Research 18-33. [CrossRef]
197. Alain DestexheCorticothalamic Feedback 184-214. [CrossRef]
198. J D Miles, K L Kilgore, N Bhadra, E A Lahowetz. 2007. Effects of ramped amplitude waveforms on the onset response of high-frequency mammalian nerve block. *Journal of Neural Engineering* **4**:4, 390-398. [CrossRef]
199. Romain Brette, Michelle Rudolph, Ted Carnevale, Michael Hines, David Beeman, James M. Bower, Markus Diesmann, Abigail Morrison, Philip H. Goodman, Frederick C. Harris, Milind Zirpe, Thomas Natschläger, Dejan Pecevski, Bard Ermentrout, Mikael Djurfeldt, Anders Lansner, Olivier Rochel, Thierry Vieville, Eilif Muller, Andrew P. Davison, Sami El

Boustani, Alain Destexhe. 2007. Simulation of networks of spiking neurons: A review of tools and strategies. *Journal of Computational Neuroscience* **23**:3, 349-398. [CrossRef]

200. Bardia F. Behabadi, Bartlett W. Mel. 2007. J4 at Sweet 16: A New Wrinkle?. *Neural Computation* **19**:11, 2865-2870. [Abstract] [PDF] [PDF Plus]
201. T. Dugladze, I. Vida, A. B. Tort, A. Gross, J. Otahal, U. Heinemann, N. J. Kopell, T. Gloveli. 2007. Impaired hippocampal rhythmogenesis in a mouse model of mesial temporal lobe epilepsy. *Proceedings of the National Academy of Sciences* **104**:44, 17530-17535. [CrossRef]
202. L. Sarid, R. Bruno, B. Sakmann, I. Segev, D. Feldmeyer. 2007. Modeling a layer 4-to-layer 2/3 module of a single column in rat neocortex: Interweaving in vitro and in vivo experimental observations. *Proceedings of the National Academy of Sciences* **104**:41, 16353-16358. [CrossRef]
203. Dekel Segev, Alon Korngreen. 2007. Kinetics of two voltage-gated K+ conductances in substantia nigra dopaminergic neurons. *Brain Research* **1173**, 27-35. [CrossRef]
204. W Tesfayesus, D M Durand. 2007. Blind source separation of peripheral nerve recordings. *Journal of Neural Engineering* **4**:3, S157-S167. [CrossRef]
205. Mahmut Ozer, Lyle J. Graham, Okan Erkaymaz, Muhammet Uzuntarla. 2007. Impact of synaptic noise and conductance state on spontaneous cortical firing. *NeuroReport* **18**:13, 1371-1374. [CrossRef]
206. Mitchell Goldfarb, Jon Schoorlemmer, Anthony Williams, Shyam Diwakar, Qing Wang, Xiao Huang, Joanna Giza, Dafna Tchetchik, Kevin Kelley, Ana Vega, Gary Matthews, Paola Rossi, David M. Ornitz, Egidio D'Angelo. 2007. Fibroblast Growth Factor Homologous Factors Control Neuronal Excitability through Modulation of Voltage-Gated Sodium Channels. *Neuron* **55**:3, 449-463. [CrossRef]
207. William S. Anderson, Pawel Kudela, Jounhong Cho, Gregory K. Bergey, Piotr J. Franaszczuk. 2007. Studies of stimulus parameters for seizure disruption using neural network simulations. *Biological Cybernetics* **97**:2, 173-194. [CrossRef]
208. K OSTROUMOV. 2007. A new stochastic tridimensional model of neonatal rat spinal motoneuron for investigating compartmentalization of neuronal conductances and their influence on firing. *Journal of Neuroscience Methods* **163**:2, 362-372. [CrossRef]
209. Robert C. Cannon, Marc-Oliver Gewaltig, Padraig Gleeson, Upinder S. Bhalla, Hugo Cornelis, Michael L. Hines, Fredrick W. Howell, Eilif Muller, Joel R. Stiles, Stefan Wils, Erik De Schutter. 2007. Interoperability of Neuroscience Modeling Software: Current Status and Future Directions. *Neuroinformatics* **5**:2, 127-138. [CrossRef]
210. Sharon Crook, Padraig Gleeson, Fred Howell, Joseph Svitak, R. Angus Silver. 2007. MorphML: Level 1 of the NeuroML Standards for Neuronal Morphology Data and Model Specification. *Neuroinformatics* **5**:2, 96-104. [CrossRef]
211. Jakob Heinzle, Peter König, Rodrigo F. Salazar. 2007. Modulation of synchrony without changes in firing rates. *Cognitive Neurodynamics* **1**:3, 225-235. [CrossRef]
212. Quan Zou, Alain Destexhe. 2007. Kinetic models of spike-timing dependent plasticity and their functional consequences in detecting correlations. *Biological Cybernetics* **97**:1, 81-97. [CrossRef]
213. Federico Minneci, Mahyar Janahmadi, Michele Migliore, Natasa Dragicevic, Daniela Avossa, Enrico Cherubini. 2007. Signaling properties of stratum oriens interneurons in the hippocampus of transgenic mice expressing EGFP in a subset of somatostatin-containing cells. *Hippocampus* **17**:7, 538-553. [CrossRef]
214. Carl Gold, Darrell A. Henze, Christof Koch. 2007. Using extracellular action potential recordings to constrain compartmental models. *Journal of Computational Neuroscience* **23**:1, 39-58. [CrossRef]
215. H. Cuntz, J. Haag, F. Forstner, I. Segev, A. Borst. 2007. Robust coding of flow-field parameters by axo-axonal gap junctions between fly visual interneurons. *Proceedings of the National Academy of Sciences* **104**:24, 10229-10233. [CrossRef]
216. A.M. Kuncel, S.E. Cooper, B.R. Wolgamuth, W.M. Grill. 2007. Amplitude- and Frequency-Dependent Changes in Neuronal Regularity Parallel Changes in Tremor With Thalamic Deep Brain Stimulation. *IEEE Transactions on Neural Systems and Rehabilitation Engineering* **15**:2, 190-197. [CrossRef]
217. Stamatios N Sotiropoulos, Peter N Steinmetz. 2007. Assessing the direct effects of deep brain stimulation using embedded axon models. *Journal of Neural Engineering* **4**:2, 107-119. [CrossRef]
218. Niloy Bhadra, Emily A. Lahowetz, Stephen T. Foldes, Kevin L. Kilgore. 2007. Simulation of high-frequency sinusoidal electrical block of mammalian myelinated axons. *Journal of Computational Neuroscience* **22**:3, 313-326. [CrossRef]
219. Svjetlana Miocinovic, Jianyu Zhang, Weidong Xu, Gary S. Russo, Jerrold L. Vitek, Cameron C. McIntyre. 2007. Stereotactic neurosurgical planning, recording, and visualization for deep brain stimulation in non-human primates. *Journal of Neuroscience Methods* **162**:1-2, 32-41. [CrossRef]

220. Izhak Michaelevski, Alon Korngreen, Ilana Lotan. 2007. Interaction of syntaxin with a single Kv1.1 channel: a possible mechanism for modulating neuronal excitability. *Pflügers Archiv - European Journal of Physiology* **454**:3, 477-494. [CrossRef]

221. Padraig Gleeson, Volker Steuber, R. Angus Silver. 2007. neuroConstruct: A Tool for Modeling Networks of Neurons in 3D Space. *Neuron* **54**:2, 219-235. [CrossRef]

222. A. E. Lindsay, K. A. Lindsay, J. R. Rosenberg. 2007. New concepts in compartmental modelling. *Computing and Visualization in Science* **10**:2, 79-98. [CrossRef]

223. Christine Voßen, Jens P. Eberhard, Gabriel Wittum. 2007. Modeling and simulation for three-dimensional signal propagation in passive dendrites. *Computing and Visualization in Science* **10**:2, 107-121. [CrossRef]

224. Hirokazu Takahashi, Masayuki Nakao, Kimitaka Kaga. 2007. Selective Activation of Distant Nerve by Surface Electrode Array. *IEEE Transactions on Biomedical Engineering* **54**:3, 563-569. [CrossRef]

225. Randall K. Weinstein, Michael S. Reid, Robert H. Lee. 2007. Methodology and Design Flow for Assisted Neural-Model Implementations in FPGAs. *IEEE Transactions on Neural Systems and Rehabilitation Engineering* **15**:1, 83-93. [CrossRef]

226. H. Kager, W. J. Wadman, G. G. Somjen. 2007. Seizure-like afterdischarges simulated in a model neuron. *Journal of Computational Neuroscience* **22**:2, 105-128. [CrossRef]

227. M. Postlethwaite, M. H. Hennig, J. R. Steinert, B. P. Graham, I. D. Forsythe. 2007. Acceleration of AMPA receptor kinetics underlies temperature-dependent changes in synaptic strength at the rat calyx of Held. *The Journal of Physiology* **579**:1, 69-84. [CrossRef]

228. Johannes K. Krottje, Arjen van Ooyen. 2007. A Mathematical Framework for Modeling Axon Guidance. *Bulletin of Mathematical Biology* **69**:1, 3-31. [CrossRef]

229. S ELBOUSTANI, M POSPISCHIL, M RUDOLPHLILITH, A DESTEXHE. 2007. Activated cortical states: Experiments, analyses and models. *Journal of Physiology-Paris* **101**:1-3, 99-109. [CrossRef]

230. Erik P. Cook, Aude C. Wilhelm, Jennifer A. Guest, Yong Liang, Nicolas Y. Masse, Costa M. ColbertThe neuronal transfer function: contributions from voltage- and time-dependent mechanisms **165**, 1-12. [CrossRef]

231. Ryota Kobayashi, Shigeru Shinomoto. 2007. State space method for predicting the spike times of a neuron. *Physical Review E* **75**:1. . [CrossRef]

232. A COHEN, J SHAPPIR, S YITZCHAIK, M SPIRA. 2006. Experimental and theoretical analysis of neuron–transistor hybrid electrical coupling: The relationships between the electro-anatomy of cultured Aplysia neurons and the recorded field potentials. *Biosensors and Bioelectronics* **22**:5, 656-663. [CrossRef]

233. T OMORI, T AONISHI, H MIYAKAWA, M INOUE, M OKADA. 2006. Estimated distribution of specific membrane resistance in hippocampal CA1 pyramidal neuron. *Brain Research* **1125**:1, 199-208. [CrossRef]

234. Michelle Rudolph, Alain Destexhe. 2006. On the Use of Analytical Expressions for the Voltage Distribution to Analyze Intracellular Recordings. *Neural Computation* **18**:12, 2917-2922. [Abstract] [PDF] [PDF Plus]

235. Robert J. Calin-Jageman, Paul S. Katz. 2006. A Distributed Computing Tool for Generating Neural Simulation Databases. *Neural Computation* **18**:12, 2923-2927. [Abstract] [PDF] [PDF Plus]

236. G MENGOV, K GEORGIEV, S PULOV, T TRIFONOV, K ATANASSOV. 2006. Fast computation of a gated dipole field. *Neural Networks* **19**:10, 1636-1647. [CrossRef]

237. Nathalie Mandairon, Casara Jean Ferretti, Conor M. Stack, Daniel B. Rubin, Thomas A. Cleland, Christiane Linster. 2006. Cholinergic modulation in the olfactory bulb influences spontaneous olfactory discrimination in adult rats. *European Journal of Neuroscience* **24**:11, 3234-3244. [CrossRef]

238. Meron Gurkiewicz, Alon Korngreen. 2006. Recording, analysis, and function of dendritic voltage-gated channels. *Pflügers Archiv - European Journal of Physiology* **453**:3, 283-292. [CrossRef]

239. M. Migliore, C. Cannia, W. W. Lytton, Henry Markram, M. L. Hines. 2006. Parallel network simulations with NEURON. *Journal of Computational Neuroscience* **21**:2, 119-129. [CrossRef]

240. Karl Farrow, Juergen Haag, Alexander Borst. 2006. Nonlinear, binocular interactions underlying flow field selectivity of a motion-sensitive neuron. *Nature Neuroscience* **9**:10, 1312-1320. [CrossRef]

241. Jie Shao, Tzu-Hsin Tsao, Robert Butera. 2006. Bursting Without Slow Kinetics: A Role for a Small World?. *Neural Computation* **18**:9, 2029-2035. [Abstract] [PDF] [PDF Plus]

242. Per Jesper Sjöström, Michael Häusser. 2006. A Cooperative Switch Determines the Sign of Synaptic Plasticity in Distal Dendrites of Neocortical Pyramidal Neurons. *Neuron* **51**:2, 227-238. [CrossRef]

243. W. R. Holmes, J. Ambros-Ingerson, L. M. Grover. 2006. Fitting experimental data to models that use morphological data from public databases. *Journal of Computational Neuroscience* **20**:3, 349-365. [CrossRef]

244. Daniel A. Nicholson, Rachel Trana, Yael Katz, William L. Kath, Nelson Spruston, Yuri Geinisman. 2006. Distance-Dependent Differences in Synapse Number and AMPA Receptor Expression in Hippocampal CA1 Pyramidal Neurons. *Neuron* **50**:3, 431-442. [CrossRef]

245. Z. Nenadic, J.W. Burdick. 2006. A Control Algorithm for Autonomous Optimization of Extracellular Recordings. *IEEE Transactions on Biomedical Engineering* **53**:5, 941-955. [CrossRef]

246. Ildiko Aradi, Péter Érdi. 2006. Computational neuropharmacology: dynamical approaches in drug discovery. *Trends in Pharmacological Sciences* **27**:5, 240-243. [CrossRef]

247. MATHILDE BADOUAL, QUAN ZOU, ANDREW P. DAVISON, MICHAEL RUDOLPH, THIERRY BAL, YVES FRÉGNAC, ALAIN DESTEXHE. 2006. BIOPHYSICAL AND PHENOMENOLOGICAL MODELS OF MULTIPLE SPIKE INTERACTIONS IN SPIKE-TIMING DEPENDENT PLASTICITY. *International Journal of Neural Systems* **16**:02, 79-97. [CrossRef]

248. Christopher R Butson, Cameron C McIntyre. 2006. Role of electrode design on the volume of tissue activated during deep brain stimulation. *Journal of Neural Engineering* **3**:1, 1-8. [CrossRef]

249. Kenji Morita, Kunichika Tsumoto, Kazuyuki Aihara. 2006. Bidirectional Modulation of Neuronal Responses by Depolarizing GABAergic Inputs. *Biophysical Journal* **90**:6, 1925-1938. [CrossRef]

250. Christopher R. Butson, Christopher B. Maks, Cameron C. McIntyre. 2006. Sources and effects of electrode impedance during deep brain stimulation. *Clinical Neurophysiology* **117**:2, 447-454. [CrossRef]

251. Kamran Diba, Christof Koch, Idan Segev. 2006. Spike propagation in dendrites with stochastic ion channels. *Journal of Computational Neuroscience* **20**:1, 77-84. [CrossRef]

252. Victoria Booth, Gina R. Poe. 2006. Input source and strength influences overall firing phase of model hippocampal CA1 pyramidal cells during theta: Relevance to REM sleep reactivation and memory consolidation. *Hippocampus* **16**:2, 161-173. [CrossRef]

253. Imre Vida, Marlene Bartos, Peter Jonas. 2006. Shunting Inhibition Improves Robustness of Gamma Oscillations in Hippocampal Interneuron Networks by Homogenizing Firing Rates. *Neuron* **49**:1, 107-117. [CrossRef]

254. Quan Zou, Yannick Bornat, Sylvain SaÏghi, Jean Tomas, Sylvie Renaud, Alain Destexhe. 2006. Analog-digital simulations of full conductance-based networks of spiking neurons with spike timing dependent plasticity. *Network: Computation in Neural Systems* **17**:3, 211-233. [CrossRef]

255. M. J. Rempe, D. L. Chopp. 2006. A Predictor#Corrector Algorithm for Reaction#Diffusion Equations Associated with Neural Activity on Branched Structures. *SIAM Journal on Scientific Computing* **28**:6, 2139-2161. [CrossRef]

256. Claus C. Hilgetag, Helen Barbas. 2005. Developmental mechanics of the primate cerebral cortex. *Anatomy and Embryology* **210**:5-6, 411-417. [CrossRef]

257. Jakob Wolfart, Damien Debay, Gwendal Le Masson, Alain Destexhe, Thierry Bal. 2005. Synaptic background activity controls spike transfer from thalamus to cortex. *Nature Neuroscience* **8**:12, 1760-1767. [CrossRef]

258. Tim Jarsky, Alex Roxin, William L Kath, Nelson Spruston. 2005. Conditional dendritic spike propagation following distal synaptic activation of hippocampal CA1 pyramidal neurons. *Nature Neuroscience* **8**:12, 1667-1676. [CrossRef]

259. Christopher R. Butson, Cameron C. McIntyre. 2005. Tissue and electrode capacitance reduce neural activation volumes during deep brain stimulation. *Clinical Neurophysiology* **116**:10, 2490-2500. [CrossRef]

260. T.M. Cickovski, Chengbang Huang, R. Chaturvedi, T. Glimm, H.G.E. Hentschel, M.S. Alber, J.A. Glazier, S.A. Newman, J.A. Izaguirre. 2005. A Framework for Three-Dimensional Simulation of Morphogenesis. *IEEE/ACM Transactions on Computational Biology and Bioinformatics* **2**:4, 273-288. [CrossRef]

261. M MOFFITT, C MCINTYRE. 2005. Model-based analysis of cortical recording with silicon microelectrodes. *Clinical Neurophysiology* **116**:9, 2240-2250. [CrossRef]

262. AMANE KOIZUMI, YUKI HAYASHIDA, TEPPEI KIUCHI, YOSHITAKE YAMADA, ATSUNORI FUJII, TETSUYA YAGI, AKIMICHI KANEKO. 2005. THE INTERDEPENDENCE AND INDEPENDENCE OF AMACRINE CELL DENDRITES: PATCH-CLAMP RECORDINGS AND SIMULATION STUDIES ON CULTURED GABAERGIC AMACRINE CELLS. *Journal of Integrative Neuroscience* **04**:03, 363-380. [CrossRef]

263. A DIMITROV. 2005. Internodal sodium channels ensure active processes under myelin manifesting in depolarizing afterpotentials. *Journal of Theoretical Biology* **235**:4, 451-462. [CrossRef]

264. A. E. Lindsay, K. A. Lindsay, J. R. Rosenberg. 2005. Increased Computational Accuracy in Multi-Compartmental Cable Models by a Novel Approach for Precise Point Process Localization. *Journal of Computational Neuroscience* **19**:1, 21-38. [CrossRef]
265. Klaus M. Stiefel, Valérie Wespatat, Boris Gutkin, Frank Tennigkeit, Wolf Singer. 2005. Phase Dependent Sign Changes of GABAergic Synaptic Input Explored In-Silicio and In-Vitro. *Journal of Computational Neuroscience* **19**:1, 71-85. [CrossRef]
266. P.B. Yoo, D.M. Durand. 2005. Selective Recording of the Canine Hypoglossal Nerve Using a Multicontact Flat Interface Nerve Electrode. *IEEE Transactions on Biomedical Engineering* **52**:8, 1461-1469. [CrossRef]
267. A. Aldo Faisal, John A. White, Simon B. Laughlin. 2005. Ion-Channel Noise Places Limits on the Miniaturization of the Brain's Wiring. *Current Biology* **15**:12, 1143-1149. [CrossRef]
268. Michael A. Sikora, Jon Gottesman, Robert F. Miller. 2005. A computational model of the ribbon synapse. *Journal of Neuroscience Methods* **145**:1-2, 47-61. [CrossRef]
269. M. D. GOLDFINGER. 2005. RALLIAN "EQUIVALENT" CYLINDERS RECONSIDERED: COMPARISONS WITH LITERAL COMPARTMENTS. *Journal of Integrative Neuroscience* **04**:02, 227-263. [CrossRef]
270. Warren M. Grill, Adam M. Simmons, Scott E. Cooper, Svjetlana Miocinovic, Erwin B. Montgomery, Kenneth B. Baker, Ali R. Rezai. 2005. Temporal excitation properties of paresthesias evoked by thalamic microstimulation. *Clinical Neurophysiology* **116**:5, 1227-1234. [CrossRef]
271. Armen Saghatelyan, Pascal Roux, Michele Migliore, Christelle Rochefort, David Desmaisons, Pierre Charneau, Gordon M. Shepherd, Pierre-Marie Lledo. 2005. Activity-Dependent Adjustments of the Inhibitory Network in the Olfactory Bulb following Early Postnatal Deprivation. *Neuron* **46**:1, 103-116. [CrossRef]
272. William W. Lytton , Michael L. Hines . 2005. Independent Variable Time-Step Integration of Individual Neurons for Network Simulations. *Neural Computation* **17**:4, 903-921. [Abstract] [PDF] [PDF Plus]
273. Jason R. Pugh, Indira M. Raman. 2005. GABAA Receptor Kinetics in the Cerebellar Nuclei: Evidence for Detection of Transmitter from Distant Release Sites. *Biophysical Journal* **88**:3, 1740-1754. [CrossRef]
274. D LEE, A JENSEN, M SCHIEFER, C MORGAN, W GRILL. 2005. Structural mechanisms to produce differential dendritic gains. *Brain Research* **1033**:2, 117-127. [CrossRef]
275. Dominique Engel, Peter Jonas. 2005. Presynaptic Action Potential Amplification by Voltage-Gated Na+ Channels in Hippocampal Mossy Fiber Boutons. *Neuron* **45**:3, 405-417. [CrossRef]
276. K. Voutsas, G. Langner, J. Adamy, M. Ochse. 2005. A Brain-Like Neural Network for Periodicity Analysis. *IEEE Transactions on Systems, Man and Cybernetics, Part B (Cybernetics)* **35**:1, 12-22. [CrossRef]
277. Gregor Wenning, Thomas Hoch, Klaus Obermayer. 2005. Detection of pulses in a colored noise setting. *Physical Review E* **71**:2. . [CrossRef]
278. G.A. Spirou, J. Rager, P.B. Manis. 2005. Convergence of auditory-nerve fiber projections onto globular bushy cells. *Neuroscience* **136**:3, 843-863. [CrossRef]
279. Chun-Hui Mo , Ming Gu , Christof Koch . 2004. A Learning Rule for Local Synaptic Interactions Between Excitation and Shunting Inhibition. *Neural Computation* **16**:12, 2507-2532. [Abstract] [PDF] [PDF Plus]
280. Geoffrey G. Murphy, Nikolai B. Fedorov, K.Peter Giese, Masuo Ohno, Eugenia Friedman, Rachel Chen, Alcino J. Silva. 2004. Increased Neuronal Excitability, Synaptic Plasticity, and Learning in Aged Kv#1.1 Knockout Mice. *Current Biology* **14**:21, 1907-1915. [CrossRef]
281. Robert W. Meech. 2004. Impulse conduction in the jellyfish Aglantha digitale. *Hydrobiologia* **530-531**:1-3, 81-89. [CrossRef]
282. Alain Destexhe, Eve Marder. 2004. Plasticity in single neuron and circuit computations. *Nature* **431**:7010, 789-795. [CrossRef]
283. A. R. Houweling. 2004. Homeostatic Synaptic Plasticity Can Explain Post-traumatic Epileptogenesis in Chronically Isolated Neocortex. *Cerebral Cortex* **15**:6, 834-845. [CrossRef]
284. N. Bhadra, K.L. Kilgore. 2004. Direct Current Electrical Conduction Block of Peripheral Nerve. *IEEE Transactions on Neural Systems and Rehabilitation Engineering* **12**:3, 313-324. [CrossRef]
285. M RUDOLPH, A DESTEXHE. 2004. Inferring network activity from synaptic noise. *Journal of Physiology-Paris* **98**:4-6, 452-466. [CrossRef]
286. D DEBAY, J WOLFART, Y LEFRANC, G LEMASSON, T BAL. 2004. Exploring spike transfer through the thalamus using hybrid artificial-biological neuronal networks. *Journal of Physiology-Paris* **98**:4-6, 540-558. [CrossRef]

287. F Veredas. 2004. A computational tool to simulate correlated activity in neural circuits. *Journal of Neuroscience Methods* **136**:1, 23-32. [CrossRef]

288. Hewerson Zansávio Teixeira, Antônio-Carlos Guimarães Almeida, Antonio Fernando Catelli Infantosi, Michelle Almeida Vasconcelos, Mário Antônio Duarte. 2004. Simulation of the effect of Na + and Cl on the velocity of a spreading depression wave using a simplified electrochemical model of synaptic terminals. *Journal of Neural Engineering* **1**:2, 117-126. [CrossRef]

289. Ruggero Scorcioni, Maciej T. Lazarewicz, Giorgio A. Ascoli. 2004. Quantitative morphometry of hippocampal pyramidal cells: Differences between anatomical classes and reconstructing laboratories. *The Journal of Comparative Neurology* **473**:2, 177-193. [CrossRef]

290. K. L. Kilgore, N. Bhadra. 2004. Nerve conduction block utilising high-frequency alternating current. *Medical & Biological Engineering & Computing* **42**:3, 394-406. [CrossRef]

291. Claude Bédard, Helmut Kröger, Alain Destexhe. 2004. Modeling Extracellular Field Potentials and the Frequency-Filtering Properties of Extracellular Space. *Biophysical Journal* **86**:3, 1829-1842. [CrossRef]

292. R Enoki. 2004. NMDA receptor-mediated depolarizing after-potentials in the basal dendrites of CA1 pyramidal neurons. *Neuroscience Research* **48**:3, 325-333. [CrossRef]

293. M.A. Moffitt, C.C. McIntyre, W.M. Grill. 2004. Prediction of Myelinated Nerve Fiber Stimulation Thresholds: Limitations of Linear Models. *IEEE Transactions on Biomedical Engineering* **51**:2, 229-236. [CrossRef]

294. CHRISTOPH S. HERRMANN, ANDREAS KLAUS. 2004. AUTAPSE TURNS NEURON INTO OSCILLATOR. *International Journal of Bifurcation and Chaos* **14**:02, 623-633. [CrossRef]

295. S Miocinovic. 2004. Sensitivity of temporal excitation properties to the neuronal element activated by extracellular stimulation. *Journal of Neuroscience Methods* **132**:1, 91-99. [CrossRef]

296. Didier Le Ray, David Fern#ndez De Sevilla, Ana Bel#n Porto, Marco Fuenzalida, Washington Bu#o. 2004. Heterosynaptic metaplastic regulation of synaptic efficacy in CA1 pyramidal neurons of rat hippocampus. *Hippocampus* **14**:8, 1011-1025. [CrossRef]

297. Philip. J. Broser, R. Schulte, S. Lang, A. Roth Fritjof, Helmchen, J. Waters, Bert Sakmann, G. Wittum. 2004. Nonlinear anisotropic diffusion filtering of three-dimensional image data from two-photon microscopy. *Journal of Biomedical Optics* **9**:6, 1253. [CrossRef]

298. Csaba Foldy, Ildiko Aradi, Allyson Howard, Ivan Soltesz. 2004. Diversity beyond variance: modulation of firing rates and network coherence by GABAergic subpopulations. *European Journal of Neuroscience* **19**:1, 119-130. [CrossRef]

299. S Kikuchi. 2003. Kinetic simulation of signal transduction system in hippocampal long-term potentiation with dynamic modeling of protein phosphatase 2A. *Neural Networks* **16**:9, 1389-1398. [CrossRef]

300. K Chono. 2003. A cell model study of calcium influx mechanism regulated by calcium-dependent potassium channels in Purkinje cell dendrites. *Journal of Neuroscience Methods* **129**:2, 115-127. [CrossRef]

301. Thomas Hoch, Gregor Wenning, Klaus Obermayer. 2003. Optimal noise-aided signal transmission through populations of neurons. *Physical Review E* **68**:1. . [CrossRef]

302. M Rudolph, A Destexhe. 2003. The discharge variability of neocortical neurons during high-conductance states. *Neuroscience* **119**:3, 855-873. [CrossRef]

303. Andreas T. Schaefer, Moritz Helmstaedter, Bert Sakmann, Alon Korngreen. 2003. Correction of Conductance Measurements in Non-Space-Clamped Structures: 1. Voltage-Gated K+ Channels. *Biophysical Journal* **84**:6, 3508-3528. [CrossRef]

304. D Heck. 2003. Passive spatial and temporal integration of excitatory synaptic inputs in cerebellar Purkinje cells of young rats. *Neuroscience Letters* **341**:1, 79-83. [CrossRef]

305. Chun-Hui Mo , Christof Koch . 2003. Modeling Reverse-Phi Motion-Selective Neurons in Cortex: Double Synaptic-Veto Mechanism. *Neural Computation* **15**:4, 735-759. [Abstract] [PDF] [PDF Plus]

306. Ron Amir, Marshall Devor. 2003. Electrical Excitability of the Soma of Sensory Neurons Is Required for Spike Invasion of the Soma, but Not for Through-Conduction. *Biophysical Journal* **84**:4, 2181-2191. [CrossRef]

307. G. Wenning, K. Obermayer. 2003. Activity Driven Adaptive Stochastic Resonance. *Physical Review Letters* **90**:12. . [CrossRef]

308. S Williams. 2003. Role of dendritic synapse location in the control of action potential output. *Trends in Neurosciences* **26**:3, 147-154. [CrossRef]

309. Daniel L. Cook, Peter C. Schwindt, Lucinda A. Grande, William J. Spain. 2003. Synaptic depression in the localization of sound. *Nature* **421**:6918, 66-70. [CrossRef]

310. J.-M Fellous, M Rudolph, A Destexhe, T.J Sejnowski. 2003. Synaptic background noise controls the input/output characteristics of single cells in an in vitro model of in vivo activity. *Neuroscience* **122**:3, 811-829. [CrossRef]
311. Alistair G Rust, Rod Adams, Maria Schilstra, Hamid BolouriEvolving computational neural systems using synthetic developmental mechanisms 353-376. [CrossRef]
312. Kevin M. Franks, Terrence J. Sejnowski. 2002. Complexity of calcium signaling in synaptic spines. *BioEssays* **24**:12, 1130-1144. [CrossRef]
313. Jing Wang, Shan Chen, Matthew F Nolan, Steven A Siegelbaum. 2002. Activity-Dependent Regulation of HCN Pacemaker Channels by Cyclic AMPSignaling through Dynamic Allosteric Coupling. *Neuron* **36**:3, 451-461. [CrossRef]
314. J.L Du, X.L Yang. 2002. Glycinergic synaptic transmission to bullfrog retinal bipolar cells is input-specific. *Neuroscience* **113**:4, 779-784. [CrossRef]
315. I Aradi. 2002. Postsynaptic effects of GABAergic synaptic diversity: regulation of neuronal excitability by changes in IPSC variance. *Neuropharmacology* **43**:4, 511-522. [CrossRef]
316. E.T. Claverol, A.D. Brown, J.E. Chad. 2002. A large-scale simulation of the piriform cortex by a cell automaton-based network model. *IEEE Transactions on Biomedical Engineering* **49**:9, 921-935. [CrossRef]
317. F. Saraga, F.K. Skinner. 2002. Dynamics and diversity in interneurons: a model exploration with slowly inactivating potassium currents. *Neuroscience* **113**:1, 193-203. [CrossRef]
318. David A. DiGregorio, Zoltan Nusser, R.Angus Silver. 2002. Spillover of Glutamate onto Synaptic AMPA Receptors Enhances Fast Transmission at a Cerebellar Synapse. *Neuron* **35**:3, 521-533. [CrossRef]
319. Boris M. Slepchenko, James C. Schaff, John H. Carson, Leslie M. Loew. 2002. COMPUTATIONAL CELL BIOLOGY: Spatiotemporal Simulation of Cellular Events. *Annual Review of Biophysics and Biomolecular Structure* **31**:1, 423-441. [CrossRef]
320. V. Krauthamer, T. Crosheck. 2002. Effects of high-rate electrical stimulation upon firing in modelled and real neurons. *Medical & Biological Engineering & Computing* **40**:3, 360-366. [CrossRef]
321. Michele Migliore, Gordon M. Shepherd. 2002. EMERGING RULES FOR THE DISTRIBUTIONS OF ACTIVE DENDRITIC CONDUCTANCES. *Nature Reviews Neuroscience* **3**:5, 362-370. [CrossRef]
322. Jens Grosche, Helmut Kettenmann, Andreas Reichenbach. 2002. Bergmann glial cells form distinct morphological structures to interact with cerebellar neurons. *Journal of Neuroscience Research* **68**:2, 138-149. [CrossRef]
323. Zhuo Wang, Dong Song, Theodore W. Berger. 2002. Contribution of NMDA receptor channels to the expression of LTP in the hippocampal dentate gyrus. *Hippocampus* **12**:5, 680-688. [CrossRef]
324. A Destexhe, M Rudolph, J.-M Fellous, T.J Sejnowski. 2001. Fluctuating synaptic conductances recreate in vivo-like activity in neocortical neurons. *Neuroscience* **107**:1, 13-24. [CrossRef]
325. Arnd Roth, Michael Hausser. 2001. Compartmental models of rat cerebellar Purkinje cells based on simultaneous somatic and dendritic patch-clamp recordings. *The Journal of Physiology* **535**:2, 445-472. [CrossRef]
326. J Feng. 2001. Is the integrate-and-fire model good enough?—a review. *Neural Networks* **14**:6-7, 955-975. [CrossRef]
327. G Lee. 2001. The double queue method: a numerical method for integrate-and-fire neuron networks. *Neural Networks* **14**:6-7, 921-932. [CrossRef]
328. Masashi Inoue, Yoshinori Hashimoto, Yoshihisa Kudo, Hiroyoshi Miyakawa. 2001. Dendritic attenuation of synaptic potentials in the CA1 region of rat hippocampal slices detected with an optical method. *European Journal of Neuroscience* **13**:9, 1711-1721. [CrossRef]
329. Jianfeng Feng, Ping Zhang. 2001. Behavior of integrate-and-fire and Hodgkin-Huxley models with correlated inputs. *Physical Review E* **63**:5. . [CrossRef]
330. Jean Chemin, Arnaud Monteil, Emmanuel Bourinet, Joël Nargeot, Philippe Lory. 2001. Alternatively Spliced #1G (CaV3.1) Intracellular Loops Promote Specific T-Type Ca2+ Channel Gating Properties. *Biophysical Journal* **80**:3, 1238-1250. [CrossRef]
331. T Miyasho. 2001. Low-threshold potassium channels and a low-threshold calcium channel regulate Ca2+ spike firing in the dendrites of cerebellar Purkinje neurons: a modeling study. *Brain Research* **891**:1-2, 106-115. [CrossRef]
332. X Lin. 2001. Computer-simulation studies on roles of potassium currents in neurotransmission of the auditory nerve. *Hearing Research* **152**:1-2, 90-99. [CrossRef]
333. GLENIS J. CRANE, MICHAEL L. HINES, TIMOTHY O. NEILD. 2001. Simulating the Spread of Membrane Potential Changes in Arteriolar Networks. *Microcirculation* **8**:1, 33-43. [CrossRef]

334. C. Meunier, I. SegevChapter 11 Neurones as physical objects: Structure, dynamics and function **4**, 353-467. [CrossRef]

335. Michael A. Arbib, Amanda Alexander, Alfredo WeitzenfeldNSL Neural Simulation Language 71-90. [CrossRef]

336. Michael A. ArbibNeuroInformatics 3-28. [CrossRef]

337. Paul H.E. Tiesinga, Jean-Marc Fellous, Jorge V. Jos#, Terrence J. Sejnowski. 2001. Computational model of carbachol-induced delta, theta, and gamma oscillations in the hippocampus. *Hippocampus* **11**:3, 251-274. [CrossRef]

338. M Migliore. 2000. A model of the effects of cognitive load on the subjective estimation and production of time intervals. *Biosystems* **58**:1-3, 187-193. [CrossRef]

339. A Destexhe. 2000. Modelling corticothalamic feedback and the gating of the thalamus by the cerebral cortex. *Journal of Physiology-Paris* **94**:5-6, 391-410. [CrossRef]

340. A Brown. 2000. Simulation of axonal excitability using a Spreadsheet template created in Microsoft Excel. *Computer Methods and Programs in Biomedicine* **63**:1, 47-54. [CrossRef]

341. A. G. Richardson, C. C. McIntyre, W. M. Grill. 2000. Modelling the effects of electric fields on nerve fibres: Influence of the myelin sheath. *Medical & Biological Engineering & Computing* **38**:4, 438-446. [CrossRef]

342. Boris V. Safronov, Matthias Wolff, Werner Vogel. 2000. Excitability of the Soma in Central Nervous System Neurons. *Biophysical Journal* **78**:6, 2998-3010. [CrossRef]

343. K. P. Carlin, K. E. Jones, Z. Jiang, L. M. Jordan, R. M. Brownstone. 2000. Dendritic L-type calcium currents in mouse spinal motoneurons: implications for bistability. *European Journal of Neuroscience* **12**:5, 1635-1646. [CrossRef]

344. Giorgio A. Ascoli. 1999. Progress and perspectives in computational neuroanatomy. *The Anatomical Record* **257**:6, 195-207. [CrossRef]

345. Li-Rong Shao, Ragnhild Halvorsrud, Lyle Borg-Graham, Johan F. Storm. 1999. The role of BK-type Ca2+-dependent K+ channels in spike broadening during repetitive firing in rat hippocampal pyramidal cells. *The Journal of Physiology* **521**:1, 135-146. [CrossRef]

346. A.M Thomson, A Destexhe. 1999. Dual intracellular recordings and computational models of slow inhibitory postsynaptic potentials in rat neocortical and hippocampal slices. *Neuroscience* **92**:4, 1193-1215. [CrossRef]

347. Alain Destexhe. 1999. Can GABAA conductances explain the fast oscillation frequency of absence seizures in rodents?. *European Journal of Neuroscience* **11**:6, 2175-2181. [CrossRef]

348. A Destexhe. 1999. Cortically-induced coherence of a thalamic-generated oscillation. *Neuroscience* **92**:2, 427-443. [CrossRef]

349. Raymond A. Chitwood, Aida Hubbard, David B. Jaffe. 1999. Passive electrotonic properties of rat hippocampal CA3 interneurones. *The Journal of Physiology* **515**:3, 743-756. [CrossRef]

350. A M. Brown. 1999. A methodology for simulating biological systems using Microsoft Excel. *Computer Methods and Programs in Biomedicine* **58**:2, 181-190. [CrossRef]

351. Cameron C. McIntyre, Warren M. Grill. 1999. Excitation of Central Nervous System Neurons by Nonuniform Electric Fields. *Biophysical Journal* **76**:2, 878-888. [CrossRef]

352. E. IGRAS, J.P. A. FOWERAKER, A. WARE, M. HULLIGER. 1998. Computer Simulation of Rhythm-Generating Networks. *Annals of the New York Academy of Sciences* **860**:1 NEURONAL MECH, 483-485. [CrossRef]

353. Ora Ohana, Bert Sakmann. 1998. Transmitter release modulation in nerve terminals of rat neocortical pyramidal cells by intracellular calcium buffers. *The Journal of Physiology* **513**:1, 135-148. [CrossRef]

354. G Shepherd. 1998. The Human Brain Project: neuroinformatics tools for integrating, searching and modeling multidisciplinary neuroscience data. *Trends in Neurosciences* **21**:11, 460-468. [CrossRef]